

Article

Changes in Extremes of Temperature, Precipitation, and Runoff in California's Central Valley During 1949–2010

Minxue He ^{1,*}, Mitchel Russo ¹, Michael Anderson ¹, Peter Fickenscher ², Brett Whitin ², Andrew Schwarz ¹ and Elissa Lynn ¹

¹ California Department of Water Resources, 1416 9th Street, Sacramento, CA 95814, USA; Mitchel.Russo@water.ca.gov (M.R.); Michael.L.Anderson@water.ca.gov (M.A.); Andrew.Schwarz@water.ca.gov (A.S.); Elissa.Lynn@water.ca.gov (E.L.)

² California-Nevada River Forecast Center, National Weather Service, 3310 El Camino Avenue, Sacramento, CA 95821, USA; Peter.Fickenscher@noaa.gov (P.F.); Brett.Whitin@noaa.gov (B.W.)

* Correspondence: Kevin.He@water.ca.gov; Tel.: +1-916-651-9634

Received: 20 November 2017; Accepted: 20 December 2017; Published: 21 December 2017

Abstract: This study presents a comprehensive trend analysis of precipitation, temperature, and runoff extremes in the Central Valley of California from an operational perspective. California is prone to those extremes of which any changes could have long-lasting adverse impacts on the society, economy, and environment of the State. Available long-term operational datasets of 176 forecasting basins in six forecasting groups and inflow to 12 major water supply reservoirs are employed. A suite of nine precipitation indices and nine temperature indices derived from historical (water year 1949–2010) six-hourly precipitation and temperature data for these basins are investigated, along with nine indices based on daily unimpaired inflow to those 12 reservoirs in a slightly shorter period. Those indices include daily maximum precipitation, temperature, runoff, snowmelt, and others that are critical in informing decision making in water resources management. The non-parametric Mann-Kendall trend test is applied with a trend-free pre-whitening procedure in identifying trends in these indices. Changes in empirical probability distributions of individual study indices in two equal sub-periods are also investigated. The results show decreasing number of cold nights, increasing number of warm nights, increasing maximum temperature, and increasing annual mean minimum temperature at about 60% of the study area. Changes in cold extremes are generally more pronounced than their counterparts in warm extremes, contributing to decreasing diurnal temperature ranges. In general, the driest and coldest Tulare forecasting group observes the most consistent changes among all six groups. Analysis of probability distributions of temperature indices in two sub-periods yields similar results. In contrast, changes in precipitation extremes are less consistent spatially and less significant in terms of change rate. Only four indices exhibit statistically significant changes in less than 10% of the study area. On the regional scale, only the American forecasting group shows significant decreasing trends in two indices including maximum six-hourly precipitation and simple daily intensity index. On the other hand, runoff exhibits strong resilience to the changes noticed in temperature and precipitation extremes. Only the most southern reservoir (Lake Isabella) shows significant earlier peak timing of snowmelt. Additional analysis on runoff indices using different trend analysis methods and different analysis periods also indicates limited changes in these runoff indices. Overall, these findings are meaningful in guiding reservoir operations and water resources planning and management practices.

Keywords: Central Valley; California; precipitation; temperature; runoff; extremes

1. Introduction

Climatic and weather-induced hazards including excessive heat, flooding, and drought are often economically, environmentally, and societally disruptive [1–3]. Previous studies have suggested that such hazards are typically caused by changes in the frequency and intensity rather than the mean of hydro-climatic variables including precipitation, temperature, and runoff [4,5]. Changes in these variables are projected to intensify in both magnitude and occurrence frequency in the future [6–9]. In light of those observations and projections, numerous studies have been dedicated to investigating the (often evolving) spatial and temporal characteristics of observed hydroclimatic extremes in areas prone to these extremes including the State of California [10–17], with the general goal being to (1) gain insights on their past behavior so that they can be better predicted in the future; and (2) inform the development of corresponding mitigation and adaptation strategies.

As the home to over 37 million people [18] and an important economy in the world, California predominantly relies on a relatively small number of big storms in the winter in the Central Valley to meet its increasing and often competing water demand during the spring and early summer [19]. A year having fewer or greater than average of such events can be particularly dry or wet. The State is thus prone to hydroclimatic extremes, with the most recent examples being water year 2015 (record high temperature and record low snowpack observed across the State) [20] and water year 2017 (record high precipitation in the Northern Sierra). Any changes to precipitation, temperature and runoff events, particularly extremes, could have long-lasting adverse impacts on the society, economy, and environment of the State. Understanding the variability and trends in these extremes is the foremost step in better predicting their future occurrence and behavior. This is particularly important in the Central Valley which serves as a major water supply source for the State. The Central Valley also accommodates the majority of the State's complex water storage and transfer system including the Central Valley Project (CVP) and State Water Project (SWP). On average, these two projects collectively provide water to about two thirds of Californians and about 15,000 km² of farmland across the State annually [21].

A number of previous studies have looked at the changes in hydroclimatic extremes in areas covering California [22–26]. The data used were typically at monthly or coarser resolution either focusing on climatic (precipitation and temperature) extremes or hydrologic (runoff) extremes. Those studies may be more meaningful in guiding long-term planning practice rather than real-time operations (e.g., providing flow forecasting to inform decisions for a short-term reservoir release schedule). The latter requires the analysis to be focused on an operational dataset (used to train or run the operational models) at temporal (sub-daily) and spatial (at forecasting basin) scales meaningful to short-term operations. Additionally, those studies generally employed the traditional linear regression approach that requires the residuals of the fitted regression line be normally distributed. This assumption is often difficult to be satisfied. Similar studies have also been conducted in regions out of California [27,28]. To our knowledge, no studies have been conducted to assess the changes in both climatic and hydrologic extremes in California, (1) at the spatial scale directly relevant to real-time water management operations; (2) using operational datasets; and (3) via a trend analysis approach other than the traditional linear regression method.

This study provides a comprehensive trend analysis of precipitation and temperature extremes for 176 major operational forecasting basins in six different forecasting groups as well as runoff extremes at 12 major water supply reservoirs in California's Central Valley. Operational long-term six-hourly precipitation and temperature along with daily inflow data for those study basins and reservoirs are used for this purpose. The study adopts a non-parametric rank-based Mann-Kendall test method with a trend-free pre-whitening procedure which requires fewer assumptions than the linear regression method. Additionally, this study investigates changes in empirical probability distributions of individual study metrics in two equal sub-periods via the two-sample Kolmogorov-Smirnov test. The study aims to address the following questions: (1) what are the direction (increasing, decreasing, or no change), rate of change, and spatial coverage of the changes in those precipitation, temperature, and runoff extremes; and (2) what are the scientific and practical implications of these changes?

2. Materials and Methods

2.1. Study Area and Dataset

This study focuses on 176 operational forecasting basins in the Central Valley (Figures 1 and A1). These basins span a wide range of elevation (with basin median elevation varying from 35 m to 3048 m) and basin size (with basin area ranging from 2.3 km² to 2782 km²) (Figure A1 and Tables A1–A6 in Appendix A). The U.S. National Weather Service California-Nevada River Forecast Center (NWS/CNRF) and California Department of Water Resources (CA DWR) jointly produce and issue short-to-long term streamflow forecasts for these basins year-round via a set of hydrologic forecasting models. These forecasts are critical to water resources managers in terms of reservoir operation, flood control, drought management, water supply planning, environment protection, and emergency response, among others.

Historical six-hourly mean areal precipitation (MAP) and mean areal temperature (MAT) data along with daily unimpaired runoff data are used to calibrate the operational forecasting models. The primary sources of MAP and MAT are point measurements of precipitation and temperature collected by Cooperative observers and archived by the National Centers for Environmental Information (NCEI). NWS hydrologists select stations and quality control the point data including consistency corrections for station moves and measurement time of day. Basin-averaging techniques for MAP are applied using PRISM climate normals [29] and station normals. The point measurements are distributed spatially and temporally into six-hourly time steps for the period of record through the MAP and MAT Preprocessors developed at the NWS Office of Hydrologic Development. Those steps generally include preliminary data checks, preliminary corrections, missing data estimate, and normalized value calculation. The readers are referred to [30] for the technical details of these analysis procedures. Daily and hourly observed streamflow from U.S. federal (e.g., United States Geological Survey, Army Corps of Engineers), state (e.g., California Department of Water Resources), and local (e.g., Kings River Water Association) agencies are applied in deriving daily unimpaired runoff for those basins. These unimpaired runoff data are archived in California Data Exchange Center (CDEC; <https://cdec.water.ca.gov/>). During every dry season, forecasters update the MAP, MAT, and daily runoff data to date for a subset of all forecasting basins and re-calibrate the forecasting models for them. The re-calibration process for all basins normally takes several years. The latest data available for all study basins are up to 2010.

This study uses six-hourly MAP and MAT data for those 176 basins from water year 1949–2010 that CNRF maintains and applies in calibration operations. Those basins belong to six forecasting groups in operations (Table 1). All the groups share a similar seasonality in precipitation (Figure 2a). It is worth noting that regional precipitation and temperature are weighted average values of individual basins based on basin size. Most of the annual precipitation (ranging from 82% of the Upper Sacramento (UPS) to 88% for the Tulare (TUL)) occurs during the wet season from November to April. The highest amount of precipitation occurs consistently in January. The wettest region is the American (AME) with a long-term mean annual precipitation of 1264 mm. In contrast, the Tulare (TUL) region receives the least amount of annual precipitation. Regarding temperature (Figure 2b), the North San Joaquin region (NSJ) is the warmest with an annual mean temperature at 12.9 °C, which is expected since a majority portion of this region is in the foothills rather the crest of the Sierra (Figure 1). In contrast, the Tulare region (TUL) has the lowest temperature given its relatively higher elevation compared to other groups (Figure 1). It is also the driest region (Figure 2a) due to its geographic location (climate tends to be drier towards the southern Valley basins).

In addition to precipitation and temperature data, daily unimpaired inflow (from CDEC) to 12 major water supply reservoirs in the Central Valley are investigated (Figure 1). The aggregated capacity of these reservoirs makes up over 44% of the total capacity of the State's 154 major reservoirs. The largest two reservoirs (Shasta Lake and Lake Oroville, in terms of capacity) serve as the major water supply sources for the Central Valley Project (CVP) and State Water Project (SWP), respectively.

The smallest reservoirs include Englebright Reservoir in the Feather-Yuba region (FYU) and Lake Success in the Tulare region (TUL) (Table 2). In terms of total annual runoff, Shasta Lake receives the largest amount on both seasonal (April–July) and annual scales, while Lake Success observes the least amount on both temporal scales. The ratio of April–July runoff over annual runoff, however, generally increases from north to south, with the exception being Lake Success which is located in the foothills (Figure 1) and is thus less impacted by snow. This indicates the increasing dominance of snow contribution to the annual runoff in the southern Sierra watersheds. Those watersheds are typically located in higher elevations (Figure 1) and thus more impacted by snow. For most reservoirs, the data record period is water year 1961–2010. For Englebright and Don Pedro, however, the data is only available in a slightly shorter period (Table 2).

Table 1. General information of six forecasting groups.

Group Name	ID	Area (km ²)	Annual Precipitation (mm) ¹	Annual Temperature (°C) ¹
Upper Sacramento	UPS	30229	940	10.3
Feather Yuba	FYU	14425	1220	9.3
American	AME	4764	1264	10.2
North San Joaquin	NSJ	5066	927	12.9
San Joaquin	SJQ	15596	884	9.9
Tulare	TUL	7622	739	8.2

¹ Annual mean value in the record period 1949–2010.

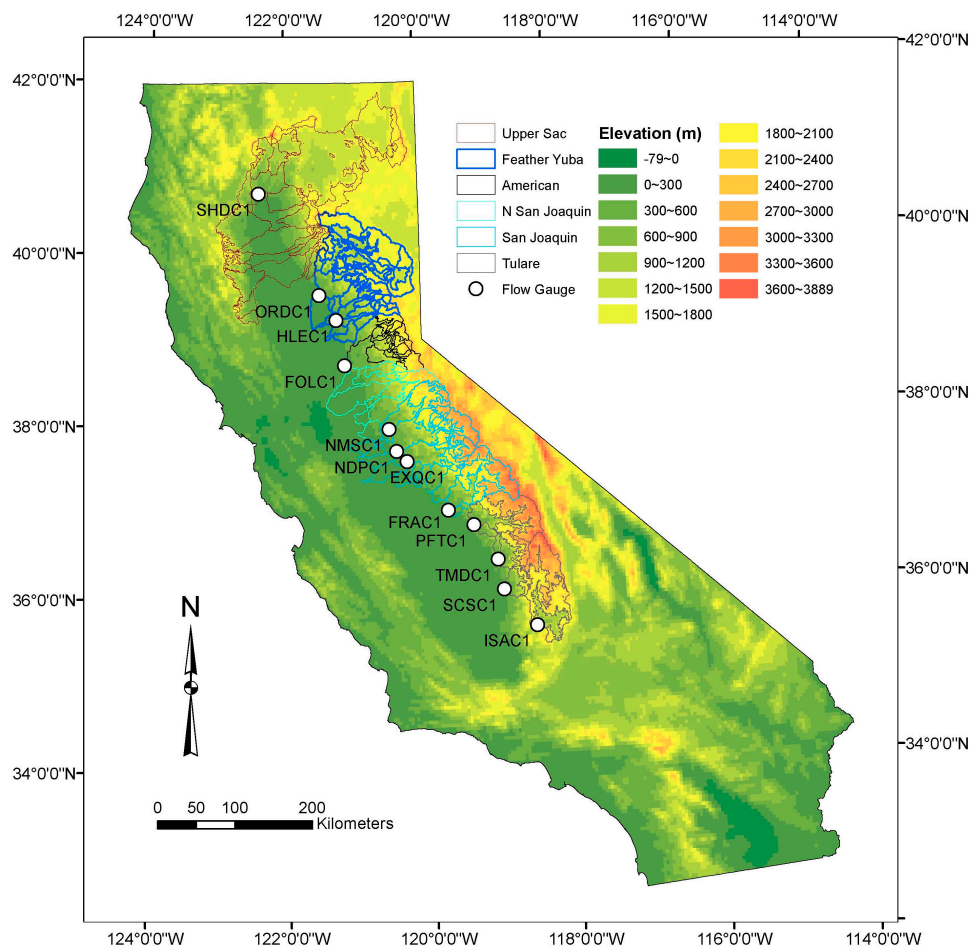


Figure 1. Location map showing study regions, basins, and reservoirs in the Central Valley of California.

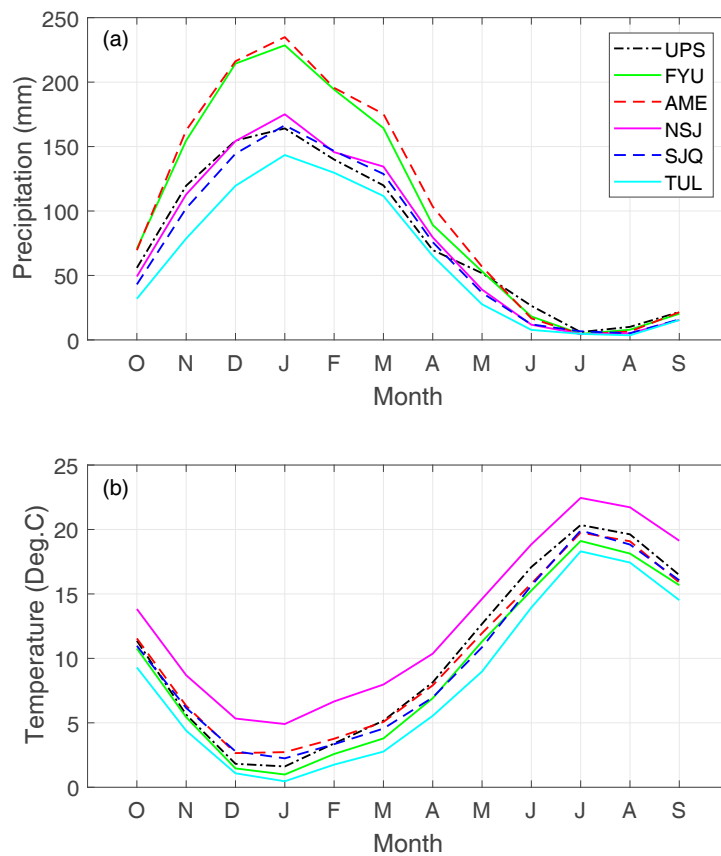


Figure 2. (a) Mean monthly precipitation and (b) mean monthly temperature of the study forecast groups for October (O), November (N), December (D), January (J), February (F), March (M), April (A), May (M), June (J), July (J), August (A), and September (S). Period of record is from water year 1949–2010.

Table 2. General information of study reservoirs.

Reservoir Name	ID	Reservoir Capacity (10 ⁹ m ³)	Drainage Area (km ²)	Unimpaired Inflow			Record Period (Water Year)
				April–July ¹ (AJ, 10 ⁹ m ³)	Annual ¹ (A, 10 ⁹ m ³)	Ratio (AJ/A)	
Shasta Lake	SHDC1	5.61	16630	2.24	7.38	0.30	1961–2010
Lake Oroville	ORDC1	4.36	9352	1.96	5.19	0.38	1961–2010
Englebright Reservoir	HLEC1	0.09	2836	1.16	2.73	0.42	1970–2010
Folsom Lake	FOLC1	1.21	4856	1.48	3.32	0.45	1961–2010
New Melones Reservoir	NMSC1	2.96	2341	0.84	1.44	0.58	1961–2010
Don Pedro Reservoir	NDPC1	2.50	3970	1.49	2.38	0.63	1971–2010
Lake McClure	EXQC1	1.26	2686	0.77	1.22	0.63	1961–2010
Millerton Lake	FRAC1	0.64	4242	1.55	2.26	0.69	1961–2010
Pine Flat Reservoir	PFTC1	1.23	4105	1.53	2.14	0.72	1961–2010
Lake Kaweah	TMDC1	0.23	1436	0.36	0.56	0.64	1961–2010
Lake Success	SCSC1	0.10	1006	0.08	0.18	0.44	1961–2010
Lake Isabella	ISAC1	0.70	5309	0.57	0.90	0.63	1961–2010

¹ Mean value in the record period.

2.2. Study Indices

The indices investigated in this study include nine indices for each variable of temperature, precipitation, and runoff (Table 3). The temperature and precipitation indices are fairly standard indices defined by the World Meteorological Organization Commission for Climatology and the Expert Team on Climate Change Detection, Monitoring, and Indices (ETCCDMI) [31]. They have been widely applied in analyzing extreme events worldwide [12,14,15,17,32–35]. The runoff indices selected are typically used as operational metrics in guiding reservoir operations and water supply planning

practices [36]. The snowmelt related indices (S1D, S3D, S5D, and SP) are determined from runoff observations from April–July which is typically deemed as the major snowmelt period in California. The timing of the center of mass of the annual runoff (QC) is calculated as a flow-weighted timing following [37,38]:

$$QC = \frac{\sum q_i t_i}{\sum q_i} \quad (1)$$

where t_i ($i = 1, 2, 3, \dots, n$; $n = 365$ for normal years and 366 for leap years) is timing in days since the start of the water year; q_i is the corresponding runoff observation for day i .

Table 3. Study indices.

Variable	Index	Description	Unit
Temperature	TX6h	Annual maximum six-hour temperature	°C
	TN6h	Annual minimum six-hour temperature	°C
	TXM	Annual mean of daily maximum temperature (TX6h)	°C
	TNM	Annual mean of daily minimum temperature (TN6h)	°C
	DTR	Annual mean of diurnal temperature range	°C
	TX10	Cold days (with TX below 10th percentile temperature)	days
	TX90	Warm days (with TX above 90th percentile temperature)	days
	TN10	Cold nights (with TN below 10th percentile temperature)	days
	TN90	Warm nights (with TN above 10th percentile temperature)	days
	Precipitation	R10	Annual count of days with precipitation above 10 mm
R20		Annual count of days with precipitation above 20 mm	days
R6h		Annual maximum six-hour precipitation	mm
R1D		Annual maximum daily precipitation	mm
R3D		Annual maximum three-day precipitation	mm
R5D		Annual maximum five-day precipitation	mm
R95		Annual count of precipitation above 95th percentile	mm
R99		Annual count of precipitation above 99th percentile	mm
SDII		Annual precipitation divided by number of wet days ¹	mm
Runoff		Q1D	Annual maximum daily runoff
	Q3D	Annual maximum three-day runoff	m ³ /s
	Q5D	Annual maximum five-day runoff	m ³ /s
	S1D	Annual maximum snowmelt runoff	m ³ /s
	S3D	Annual maximum three-day snowmelt runoff	m ³ /s
	S5D	Annual maximum five-day snowmelt runoff	m ³ /s
	QP	Peak runoff day	DOWY ²
	QC	Timing of the center of mass of the runoff	DOWY ²
	SP	Peak snowmelt runoff day	DOWY ²

¹ Wet days indicate the days with accumulated precipitation above 1 mm; ² DOWY designates “Day of Water Year”. For instance, DOWYs for 1st October and 1st January are 1 and 93, respectively.

2.3. Trend Analysis

There are generally two types of trend analysis methods, parametric and non-parametric [39,40], commonly applied in climatic and hydrological trend analysis. Compared to parametric methods (e.g., linear regression), the non-parametric approaches require fewer assumptions including not requiring the study data to be normally distributed. The assumptions on data distribution are often not satisfied due to a range of issues including missing data. As such, the non-parametric methods are considered more robust than the parametric ones [40]. Among the non-parametric methods, the Mann–Kendall test (MKT) [41,42] is likely the most widely used, particularly in the field of hydrology and climatology [43]. This study employs the MKT in assessing the significance of a trend. In this approach, the sign of each possible pair of observations is first identified, followed by the calculation of the corresponding test statistic δ . The null hypothesis (H_0) assumes no significant monotonic trend in the observations while the alternative hypothesis suggests otherwise. The null hypothesis is rejected when $|z| > z_{1-\alpha/2}$, where $z_{1-\alpha/2}$ is the probability of the standard

normal distribution at a significance level of α . In this study, α is set as 0.05 unless otherwise noted. The corresponding $z_{1-\alpha/2}$ equals 1.96 in this case. The non-parametric Theil–Sen approach (TSA) [44,45] is used in the study to identify the slope of significant trends determined via the MKT. The slope values (vector S) of all data pairs in the study time series are first determined:

$$S = \frac{x_i - x_j}{i - j} \quad i = 1, 2, \dots, n; j = 1, 2, \dots, n; i > j \quad (2)$$

where n is the length of the time series; x_i and x_j are time series values at time i and j , respectively, with $i > j$. The median of S is the Sen's estimate on the slope. A positive (negative) slope value indicates an increasing (decreasing) trend. A detailed explanation on the TSA method can be found at [43].

Previous research [46–48] suggested that the presence of positive serial correlation (which is common in hydroclimatic observations including temperature and runoff measurements) increases the probability of false rejection of the null hypothesis of no trends. [43,49] proposed a trend-free pre-whitening procedure (TFPW) to address the serial correlation issue. The general steps include, first, de-trending the original time series which has a significant trend (determined via the MKT with a significance level of 0.05); removing a lag-one auto-regressive process from the de-trended time series to produce a new time series; adding the trend in the original time series to the new time series, yielding a pre-whitened time series which is then used in the trend analysis. The readers are referred to [49] for technical details on the TFPW procedure.

2.4. Distribution Pattern

In addition to the trends across the entire study period, changes in empirical probability distributions of individual study indices in two equal sub-periods of the study period are also investigated. Specifically, the study period of a specific index (e.g., 1949–2010 for R10) is divided into two halves (e.g., 1949–1979 and 1980–2010). The general idea is to evaluate if there are any pronounced shifts in the statistical characteristics (e.g., median, probability distribution) of the study indices in two different phases of the study period. Two equal sub-periods (e.g., two halves of the study period) are often adopted as a common practice [30]. The empirical probability distribution functions (PDFs) of the index in these two sub-periods are derived and compared with each other. Following [32], a two-sample Kolmogorov-Smirnov test is applied to test if the index values in two sub-periods come from a same distribution (null hypothesis) or different distributions (alternative hypothesis). Specifically, the test compares the cumulative distribution functions (CDFs) of two samples in those two sub-periods, respectively. The test outputs a p -value corresponding to a critical value of the maximum absolute difference between these two CDFs. The alternative hypothesis is favored if the p -value is less than a preset significance level (0.05 in this case). More details on this method are available in [32,50].

3. Results

3.1. Temperature Indices

A variety of basins show significant trends for each of the nine temperature indices, ranging from 41 basins (for number of warm days (TX90)) to 136 basins (for annual mean minimum temperature (TNM)) out of the 176 study basins (Figure 3a). The trends in three indices including number of cold days (TX10), number of cold nights (TN10), and mean diurnal temperature range (DTR) are mostly negative, indicative of decreasing number of cold days, cold nights, and decreasing daily temperature range for those basins. For warm days (TX90), about half of the basins (22 out of 41) showing significant changing tendency have increasing trends. For the remaining five indices, the trends are generally positive, suggesting that the number of warm nights (TN90), six-hourly maximum (TX6h) and minimum (TN6h) temperature, and annual mean maximum (TXM) and minimum (TNM) temperature are all increasing for those basins that exhibit significant trends. The relationship between

these trend slopes and basin elevations is moderate for the number of cold days (TX10, with a Pearson's correlation coefficient at 0.53 and $p = 0.002$) and minimum six-hourly temperature (TN6h, with a correlation coefficient at 0.57 and $p = 0$), indicating basins in higher elevations have a relatively stronger increasing trend in these two indices. For other indices, the correlation is generally not strong (Figure 3a), neither is the relationship between these trend slopes and the geographic location (latitude and longitude) of the study basins (not shown). It is worth noting that there are a few basins showing increasing trends in cold days (TX10) and diurnal temperature range (DTR) as well as decreasing warm nights (TN90) and annual mean maximum temperature (TXM). However, these basins only account for a very small percentage of the entire study area (1.3% for TX10, 1.9% for TN90, 1.6% for TXM, and 1.7% for DTR). Nevertheless, the inconsistent responses across different basins to the changing climate highlight the complex geographic conditions of these basins (Tables A1–A6). Looking at the overall percentage of area showing significant trend (Figure 3b), slightly above 60% of the total area of the 176 study basins exhibits increasing trend for number of warm nights (TN90), maximum six-hourly temperature (TX6h), and annual mean minimum temperature (TNM). There is roughly 60% of the total area showing decreasing trend in the number of cold nights (TN10). About half of the area observes increasing minimum six-hourly temperature (TN6h), while the basins showing a smaller daily diurnal temperature ranges also accounts for about half of the total area. For the remaining indices, the area with either increasing or decreasing trend accounts for less than one third of the total area.

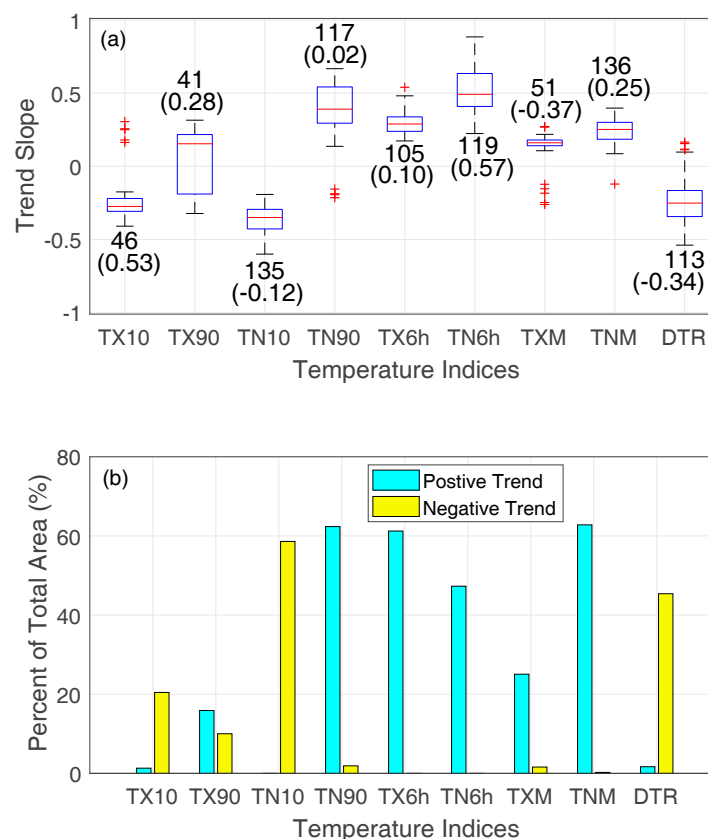


Figure 3. (a) Slope of significant trend of temperature indices at basin-scale in the study period 1949–2010. The unit of the slope for the first four indices (TX10, TX90, TN10 and TN90) is days/year; for other indices, the unit is °C/decade. The numbers in parentheses represent the correlation values between the slope and basin elevation; the numbers above these correlation values designate the sample size (i.e., number of basins showing significant trends). (b) Aggregated area of basins showing negative or positive trends over the total area of all 176 study basins.

On the regional scale (Figure 4), all six regions exhibit significant increasing trend in the annual mean minimum temperature (TNM). All regions except for the Upper Sacramento region (UPS) show significant decreasing trend (with changing rate ranging from -0.44 to -0.31 day/year) in the number of cold nights (TN10) and increasing trend (with trend slope varying from 0.26 to 0.56 day/year) number of warm nights (TN90). Those five regions also observe decreasing (with rate varying from -0.31 to -0.13 °C/decade) diurnal temperature range (DTR). Five out of six regions (except for North San Joaquin) also show increasing tendency in maximum six-hourly temperature (TX6h). Across all regions, Tulare (TUL) is the only one exhibiting significant trends in all nine temperature indices, highlighting its sensitivity to temperature change. Except for Tulare region, the other five regions show no significant changes in the number of cold days (TX10), warm days (TX90), and annual mean maximum temperature (TXM).

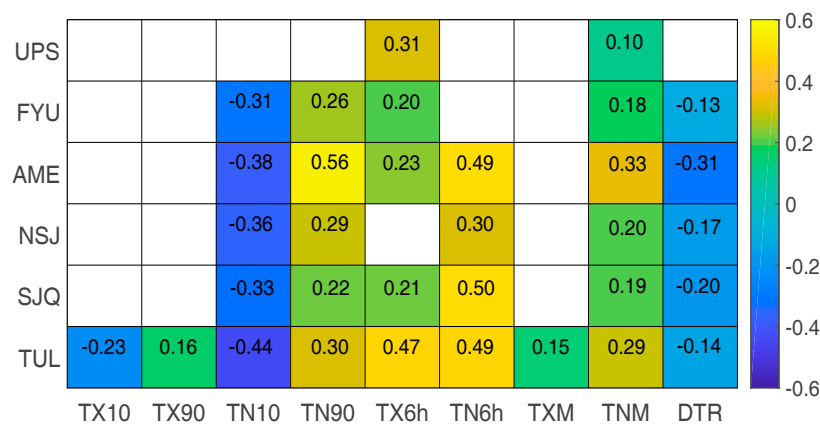


Figure 4. Slope of significant trend of temperature indices at regional (forecasting group) scale in the study period 1949–2010. Slope unit is day/year for TX10, TX90, TN10 and TN90; for other indices, the unit is °C/decade. White color indicates that there is no significant trend. Slope values of significant decreasing trends are provided.

Different basins show significantly different distribution patterns in the first half and second half (hereinafter referred to as “two sub-periods”) of the study period across different temperature indices (Figure 5). More than half of the study area shows different distributions for four indices including number of cold nights (TN10) and warm nights (TN90), minimum six-hourly temperature (TN6h), and the annual mean of minimum temperature (TNM). Specifically, 77% of the study area has different TNM distributions in two sub-periods of the entire study period (Figure 5i). For these four indices, their corresponding study areas exhibiting significant trend are also high (around 60%, Figure 3b). The index with the smallest amount of area (9%) showing different distributions in two sub-periods is the number of warm days (TX90; Figure 5b). This confirms the observation in Figure 3 that changes in this index are the least consistent among all indices. Particularly, for the basins with significant trend in this index, about half of them have increasing trend and the other half show negative trends (Figure 3b). For the remaining four indices, the area showing different distributions in two sub-periods accounts for about 23% (number of cold nights, TX10) to 38% (annual mean maximum temperature, TXM).

Looking at differences in distribution patterns in the two sub-periods at the regional scale, annual mean minimum temperature (TNM) is the only index showing significant differences across all six study regions (Figure 6), with the p -value ranging from near zero (TUL) up to 0.01 (UPS). It is also the only index exhibiting significant trends for all regions (Figure 4). In contrast, the number of warm days (TX90) tends to preserve the same distribution in two sub-periods for all regions. For the number of cold nights (TN10) and minimum six-hourly temperature (TN6h), five out of six regions have significant differences in distribution patterns in two sub-periods. Across all study regions, Tulare region (TUL) again shows most significant changes with eight out of nine indices having significantly different distribution patterns in two sub-periods.

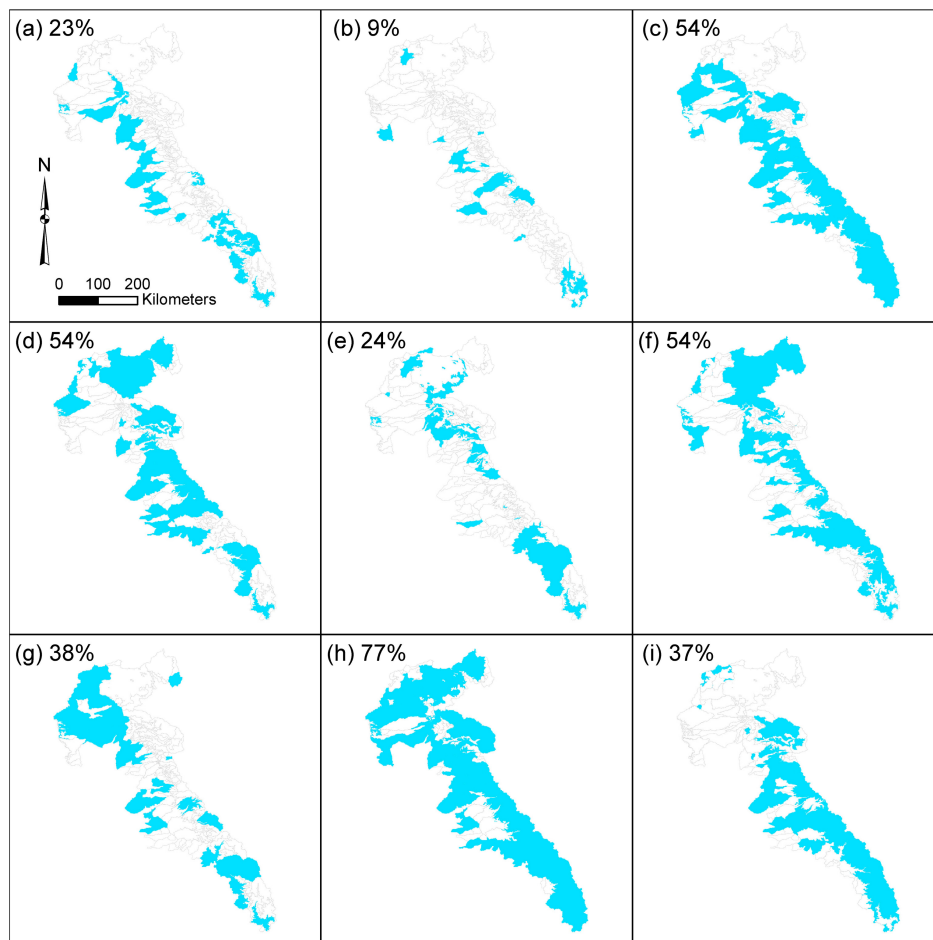


Figure 5. Study basins (highlighted in blue) with significantly (at a significance level of 0.05) different probability distributions in two different sub-periods of the study period for temperature indices (a) TX10, (b) TX90, (c) TN10, (d) TN90, (e) TX6h, (f) TN6h, (g) TXM, (h) TNM, and (i) DTR. Percentage numbers show how much the aggregated area of those basins accounts for the entire study area.

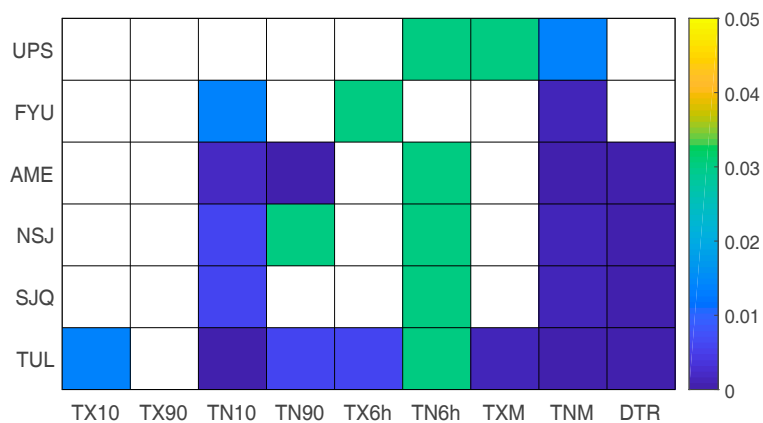


Figure 6. *p*-Values of the Kolmogorov-Smirnov test for nine temperature indices in the study period from water year 1949–2010. White color indicates that the null hypothesis (index in two sub-periods comes from the same distribution) is favored (*p*-value > 0.05).

The probability distributions of those indices in two sub-periods are further explored for the Tulare region (TUL) (Figure 7). It is evident that, except for TX90 index (number of warm days; Figure 7b), other indices have remarkable shifts in the distributions in two sub-periods. This is consistent with the observation in Figure 6 that TX90 is the only index with a p -value (0.12) greater than 0.05. Among other indices, minimum six-hourly temperature (TN6h) has the highest p -value (0.03). Compared to the first sub-period (1949–1979), the second sub-period (1980–2010) observes less number of cold days (TX10; Figure 7a) and cold nights (TN10; Figure 7c) on average, while it has higher number of warm nights (TN90; Figure 7d). Meanwhile, the second sub-period generally has higher maximum (TX6h; Figure 7e) and minimum (TN6h; Figure 7f) six-hourly temperature as well as higher annual mean maximum (TXN; Figure 7g) and minimum (TNM; Figure 7h) temperature. Those observations collectively indicate a transition to more warming conditions in the recent decades (1980–2010). The second sub-period also has a smaller diurnal temperature range (DTR; Figure 7i) compared to the first sub-period, implying that the daily minimum temperature is increasing at a faster rate than the daily maximum temperature.

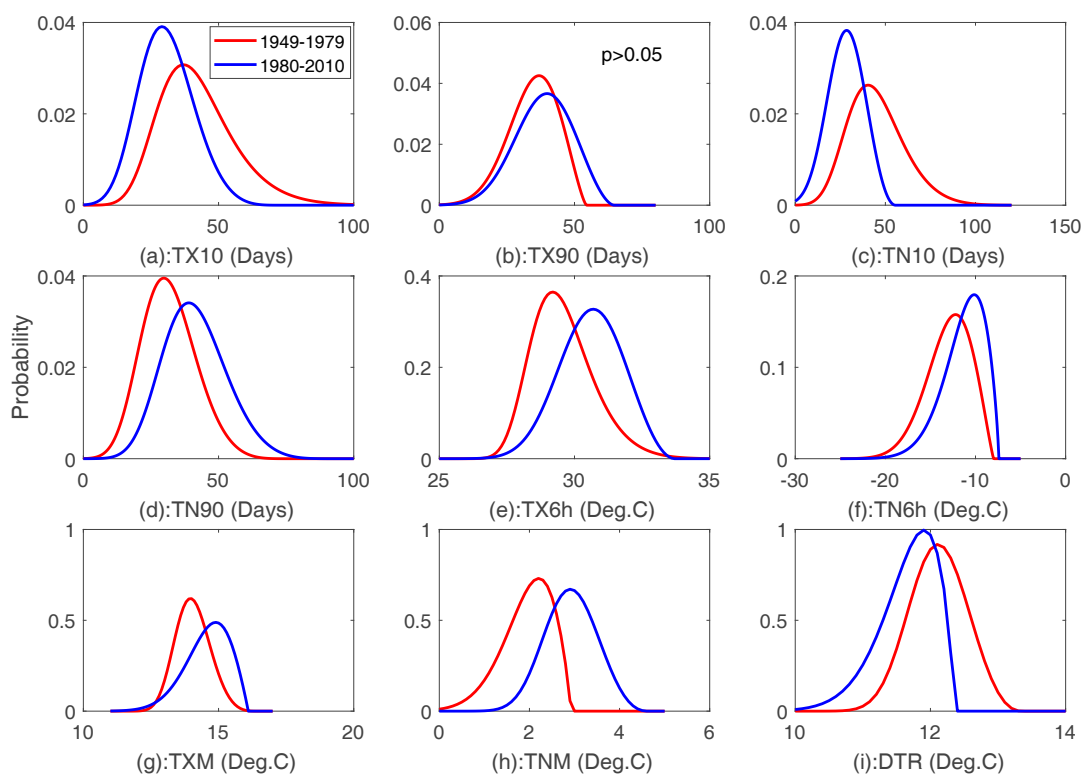


Figure 7. Probability Distribution Functions of nine temperature indices (a) TX10, (b) TX90, (c) TN10, (d) TN90, (e) TX6h, (f) TN6h, (g) TXM, (h) TNM, and (i) DTR in two sub-periods: water year 1949–1979 (red line) and 1980–2010 (blue line) for the Tulare region (TUL).

3.2. Precipitation Indices

For precipitation, only four out of nine investigated indices show significant trend in a certain number of basins (Figure 8). Specifically, only four basins that account for 1.6% of the total study area exhibit decreasing trend in maximum six-hour precipitation (R6h; Figure 8a). The decreasing rate is generally small, ranging from -0.15 mm/year to -0.10 mm/year. There are 11 basins (7.5% of the entire study area) showing decreasing trend in maximum daily precipitation (R1D), with trend slope ranging from -0.47 mm/year to -0.24 mm/year (Figure 8b). There is only one basin (1% of the study area) showing significant declining tendency in 99th percentile precipitation (R99). As for the simple daily intensity index (SDII), 23 basins (9.3% of the study area) exhibit decreasing tendency (Figure 8d). However, the decreasing rate is not remarkable in terms of magnitude. The correlation coefficient between

the slope value of R1D (SDII) and basin median elevation is -0.62 with $p = 0.04$ (-0.64 with $p = 0.001$), indicative of a milder decreasing rate for high elevations for those basins exhibiting significant trends.

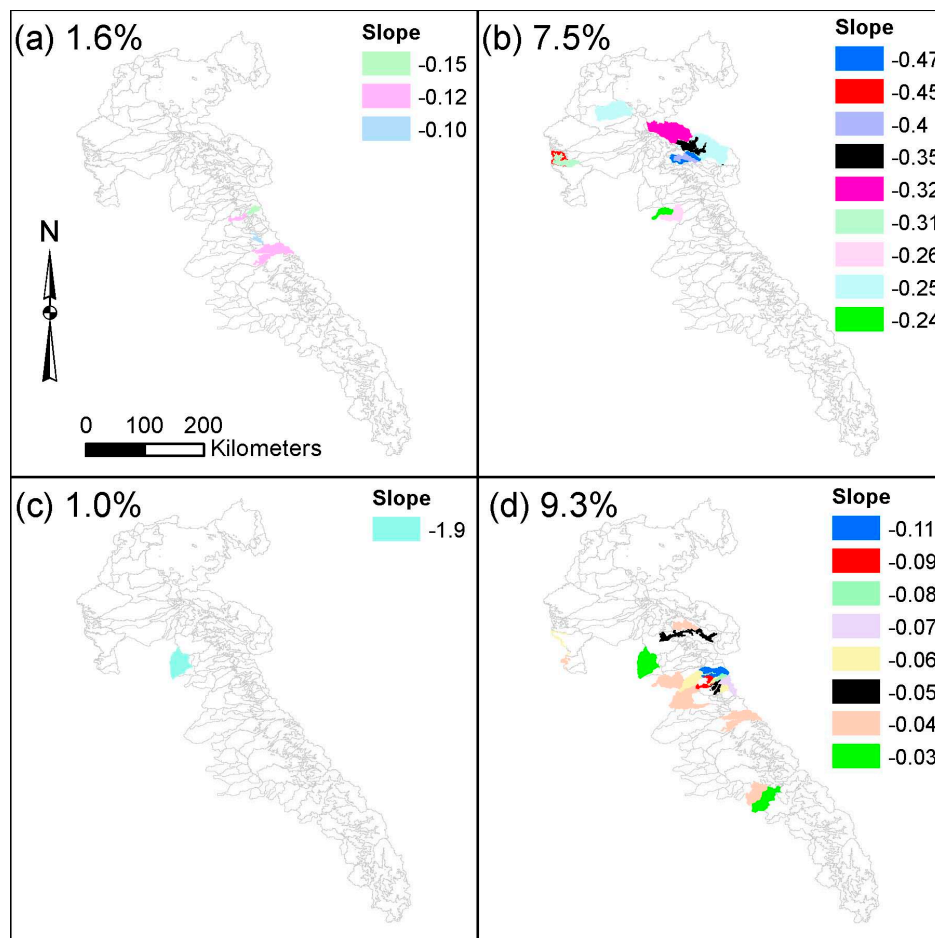


Figure 8. Study basins with significant (at a significance level of 0.05) trend in precipitation indices (a) R6h, (b) R1D, (c) R99, and (d) SDII. Other precipitation indices show no significant trend in any study basins. Different colors indicate different trend slopes (in mm/year). Percentages show how much the aggregated area of those basins (with significant trend) accounts for the entire study area.

Looking at the regional scale, generally all regions show a declining tendency in maximum six-hourly (T6h), daily (R1D), three-day (R3D), and 99th percentile precipitation (R99) as well as the simply daily intensity index (SDII) (Table 4). However, only the trends in R6h and SDII for American region (AME) are significant ($\alpha = 0.05$). In both cases, the decreasing rates are generally small (-0.11 mm/year and -0.05 mm/year, respectively).

Table 4. Trend slope of precipitation indices at the regional scale ¹.

ID	R10	R20	R6h	R1D	R3D	R5D	R95	R99	SDII
UPS	0	0	-0.02	-0.16	-0.15	-0.10	-0.27	-0.51	-0.01
FYU	0	-0.03	-0.02	-0.23	-0.34	-0.39	-2.60	-1.48	-0.03
AME	0.03	-0.03	-0.11	-0.27	-0.42	-0.55	-2.85	-1.50	-0.05
NSJ	0	0	-0.06	-0.13	-0.12	-0.18	-0.37	-0.74	-0.02
SJQ	0.02	0	-0.03	-0.12	0.00	0.06	0.05	-0.80	-0.01
TUL	0.03	0	-0.03	-0.16	-0.15	-0.05	0.23	-0.45	-0.03

¹ Trend slope unit is mm/year. Significant ($\alpha = 0.05$) trends are highlighted in bold.

The distribution patterns in two sub-periods for those precipitation indices are also investigated. Unlike their temperature counterparts, those indices show no significant shifts in distributions for any basin or any region (p -value consistently above 0.05). All in all, the changes in precipitation extremes are generally insignificant in terms of change rate and spatially incoherent.

3.3. Runoff Indices

In addition to precipitation and temperature indices, this study further investigates the changes in runoff indices since runoff, as opposed to precipitation and temperature, is often the variable directly used to inform decision making in most water resources planning and management practices. Surprisingly, none of the 12 locations exhibit any statistically significant (at 0.05 significance level) in peak volume indices (including maximum daily, three-day, and five-day runoff and snowmelt) and the timing indices (QP, QC, and SP). Only Lake Isabella (ISAC1) shows significant decreasing trend in peak snowmelt timing (occurs earlier at a rate about 0.23 day/year) when the significant level is slightly increased (using 0.06 instead of 0.05 as the significance level). With an even higher significance level (0.10), one additional location (Folsom Lake, FOLC1) shows significant trend in peak runoff timing (occurs later at a rate of 1 day/year). This is likely due to the decreasing tendency observed in most precipitation extremes (Table 4) in the American region (AME) which drains into Folsom Lake. For other indices and other locations, no significant trends are detected at this significant level (0.10).

Looking at index PDFs in two sub-periods of the record period, it is largely unlikely to favor the hypothesis that the index in two sub-periods comes from two different distributions only with one exception (peak snowmelt timing for Lake Isabella; Table 5). This is likely due to the fact that its drainage basins are the most southern ones (drier conditions are typically expected moving south). Snowmelt makes up a large contribution to runoff at this location (April–July runoff accounts for 63% of the annual runoff; Table 2). While snowmelt is very sensitive to warming, no significant changes in precipitation extremes are observed (Figure 8). In brief, changes in runoff extremes are even less significant and consistent (spatially) compared to changes in precipitation indices.

Table 5. p -Value of the KS test on runoff indices ¹.

ID	Q1D	Q3D	Q5D	S1D	S3D	S5D	QP	QC	SP
SHDC1	0.88	0.88	0.65	0.88	0.88	0.65	0.41	0.24	0.12
ORDC1	0.65	0.88	0.65	0.99	0.99	0.88	0.65	0.99	0.41
HLEC1	0.98	0.85	0.84	0.41	0.71	0.81	0.96	0.08	0.89
FOLC1	0.88	0.88	0.88	0.88	0.65	0.88	0.12	0.24	0.65
NMSC1	0.41	0.24	0.24	0.41	0.41	0.41	0.65	0.99	0.88
NDPC1	0.77	0.77	0.77	0.50	0.50	0.77	0.77	0.28	0.50
EXQC1	0.65	0.88	0.88	0.99	0.99	0.99	0.12	0.99	0.88
FRAC1	0.65	0.88	0.99	0.99	0.99	0.99	0.12	0.88	0.06
PFTC1	0.88	0.65	0.99	0.99	0.99	0.99	0.41	0.88	0.65
TMDC1	0.88	0.88	0.65	0.99	0.88	0.88	0.88	0.99	0.24
SCSC1	0.65	0.65	0.88	0.24	0.41	0.65	0.12	0.65	0.24
ISAC1	0.88	0.41	0.65	0.65	0.65	0.88	0.24	0.65	0.03

¹ The null hypothesis (no change in distribution) is favored when p -value > 0.05.

4. Summary and Discussions

4.1. Temperature Indices

The results show significant decreasing trend in the number of cold nights (TN10) along with increasing trends in the number warm nights (TN90), maximum six-hourly temperature (TX6h), and annual mean minimum temperature (TNM) for about 60% of the entire study area. At the regional scale, changes in these indices are also evident. Specifically, all six study regions show increasing trends in annual mean minimum temperature (TNM) and five regions exhibit significant trend in cold nights

(TN10; decreasing trend), warm nights (TN90; increasing trend), and maximum six-hourly temperature (TX6h; increasing trend). This transition toward more warm extremes has also been noticed in previous studies in other regions around the world [17,32–34,51]. The current study further identifies decreasing trends in diurnal temperature range (DTR) at both basin (statistically significant at about half of the entire study area) and regional (significant over five out of six regions) scales. This finding was also reported in previous studies [10,16,33,35]. This decreasing trend is likely due to the fact that increasing trend observed in annual mean maximum temperature (TXM) is not as significant (in terms of change rate) and consistent (in terms of area exhibiting trends) as that of the annual mean minimum temperature (TNM). The correlation between the changing rate and the elevation of the corresponding basin (exhibiting changes) is generally not strong. There are remarkable shifts in the empirical probability distribution functions (PDFs) in the first half (1949–1979) of the study period and second half (1980–2010) of the study period over half of the entire study area for the number of cold nights (TN10), warm nights (TN90), minimum six-hourly temperature (TN6h), and annual mean minimum temperature (TNM), indicating more warming conditions in the second half of the study period. Comparing different regions, Tulare region (TUL) preserves the most consistent changes measured by both trend (all nine indices show significant warming tendency) and PDFs pattern change (eight out of nine indices with PDFs shifts toward warming conditions in the second half of the study period). This is not surprising given its elevation (highest and thus coolest region) and geographic location (most southern and thus driest region) which make it the region most sensitive to any changes in temperature extremes.

4.2. Precipitation Indices

In contrast to temperature indices, precipitation indices show much less significant and coherent changes. Five indices including annual count of heavy precipitation days (R10) and very heavy precipitation days (R20), maximum three-day (R3D) and five-day precipitation (R5D), along with annual count of precipitation above 95th percentile (R95) show no significant increasing or decreasing trends at any of the 176 study basins. Only four basins (1.6% of the entire study area) show statistically significant decreasing trend in maximum six-hourly precipitation (R6h) and only one basin (1% of the study area) has decreasing trend in the 99th percentile precipitation (R99). A slightly larger number of basins (11; 7.5% of the study area) exhibits decreasing tendency in maximum daily precipitation (R1D). However, the decreasing rates are generally small. Decreasing trends are also observed in the simple daily precipitation intensity index (SDII) for 23 basins (9.3% of the study area). At the regional scale, most regions show weak and insignificant trends for most indices. Only one region (American) observes statistically significant decreasing trend in two indices. When comparing the PDFs of these indices in two halves of the study periods, no basins or regions show remarkable shifts in the distribution pattern. Lack of strong (in terms of changing rate) and consistent (spatially) changes in precipitation has also been reported in previous work [11,33,52,53]. In general, this observation implies that natural variability in precipitation may still dominate the influence of climate change, which is most likely the case in the current study given the fact that California has the largest year-to-year natural variability in precipitation across the United States [19].

4.3. Runoff Indices

In another finding, this study identifies that there are generally no significant changes in peak volume and timing of runoff and snowmelt draining into 12 major water supply reservoirs in the Central Valley, with the sole exception being the peak snowmelt timing for Lake Isabella. This is somewhat contradictory to previous studies on changes in runoff in the Western United States [37,38,54–57] that noted increasing fractions of annual runoff occurring earlier than usual in the water year and earlier occurrence of snowmelt peak. This discrepancy likely stems from the fact that the study methods, study locations, study data, and record period of the current work are not necessarily included in those previous studies. Additionally, the pre-whitening procedure [43] applied in this study may mask potential trend in the raw data. To test this assumption, the Mann-Kendall test (MKT) approach without pre-whitening is applied to those runoff indices. Moreover, to illustrate how differently the MKT method performs from the traditional

method, the linear regression method is also utilized in identifying the significance of the linear slope identified for those indices. The resulting z -value from the MKT and the p -value from the linear regression are tabulated in Tables 6 and 7, respectively. Additionally, to assess the potential influence of the length of study period on the results, both the MKT and traditional linear regression methods are applied in every single 30-year sub-period within the record period of the study indices. A 30-year window is applied to allow enough sample size (30) for trend analysis. The number of 30-year windows showing statistically significant changes at a significance level of 0.05 are counted and tabulated in Table 8.

The MKT results (Table 6) are identical with those of the coupled MKT and the trend-free pre-whitening approach. There are no significant trends detected by the MKT method at a significance of 0.05. However, the peak snow melt timing for Lake Isabella (ISAC1) and the peak runoff timing for Folsom Lake (FOLC1) show trends at a significance level of 0.10. This observation implies that the serial correlation between annual runoff extremes may not be strong. Addition of the pre-whitening procedure does not change the trend analysis results.

Table 6. z -Value of the MKT on runoff indices ¹.

ID	Q1D	Q3D	Q5D	S1D	S3D	S5D	QP	QC	SP
SHDC1	−0.59	−0.52	−0.55	0.33	0.07	−0.12	−0.23	1.57	1.33
ORDC1	−0.20	−0.54	−0.59	0.10	0.00	−0.10	0.51	0.45	0.24
HLEC1	−0.46	−0.24	−0.30	0.64	0.35	0.55	0.53	1.29	−0.70
FOLC1	−0.45	−0.17	−0.23	0.62	0.25	0.30	1.87	1.56	0.80
NMSC1	−0.18	−0.40	−0.55	−0.08	−0.13	−0.20	0.07	−0.55	0.03
NDPC1	0.76	0.64	0.55	1.13	0.90	0.62	0.52	0.50	−1.33
EXQC1	−0.08	0.12	0.27	0.92	0.95	0.72	1.61	0.42	−0.31
FRAC1	0.25	0.57	0.70	0.90	0.95	0.87	0.70	0.07	−1.20
PFTC1	0.40	0.55	0.85	1.10	0.92	0.95	0.92	−0.18	−0.32
TMDC1	−0.03	0.07	0.22	0.77	0.64	0.59	−0.57	0.18	−1.45
SCSC1	−0.30	−0.35	−0.12	−0.16	−0.20	−0.17	1.09	0.74	0.43
ISAC1	0.10	0.25	0.38	0.50	0.50	0.59	0.13	0.12	− 1.89

¹ Those with significant trends at a significance value of 0.10 are highlighted in bold.

The linear regression results (Table 7) are generally in line with those of the MKT method with a few exceptions. Particularly, the trend of peak inflow to Lake Folsom is significant ($p = 0.02$). When a higher significance level (0.10) is applied, Millerton Lake (FRAC1) inflow shows significant trend (occurs later at about 1 day/year) in addition to the peak snow melt timing of Lake Isabella (occurs earlier at about 0.24 day/year). However, the linear regression method requires normality in the data, while runoff extremes are not normally distributed in nature. The non-parametric MKT approach is considered more robust [58,59] in assessing trend in streamflow data.

Table 7. p -Value of estimated trend slope of runoff indices via linear regression ¹.

ID	Q1D	Q3D	Q5D	S1D	S3D	S5D	QP	QC	SP
SHDC1	0.49	0.54	0.58	0.84	0.99	0.94	0.79	0.17	0.29
ORDC1	0.86	0.66	0.65	0.61	0.81	0.94	0.47	0.50	0.98
HLEC1	0.84	0.74	0.70	0.44	0.42	0.39	0.21	0.22	0.51
FOLC1	0.65	0.51	0.51	0.22	0.37	0.41	0.02	0.12	0.30
NMSC1	0.68	0.55	0.53	0.84	0.89	0.71	0.83	0.57	0.93
NDPC1	0.62	0.77	0.80	0.40	0.53	0.58	0.40	0.71	0.30
EXQC1	0.62	0.88	0.99	0.47	0.43	0.55	0.10	0.92	1.00
FRAC1	0.96	0.74	0.52	0.50	0.53	0.49	0.08	0.86	0.30
PFTC1	0.59	0.87	0.52	0.54	0.52	0.49	0.19	0.80	0.79
TMDC1	0.15	0.25	0.37	0.75	0.72	0.73	0.53	0.87	0.24
SCSC1	0.17	0.24	0.27	0.99	0.99	0.96	0.38	0.38	0.77
ISAC1	0.20	0.33	0.47	1.00	0.99	0.97	0.60	0.96	0.07

¹ Those with significant trends at a significance level of 0.10 are highlighted in bold.

The influence of different analysis periods on the trend analysis results are generally marginal, as indicated by the limited amount of 30-year sub-periods showing significant changes (Table 8). Specifically, neither the MKT method nor the linear regression method identifies any significant change in any 30-year sub-period for the maximum one-day (Q1D), three-day (Q3D), and five-day (Q5D) runoff (Table 8). Additionally, no statistically significant changes in the maximum one-day (S1D), three-day (S3D), and five-day (S5D) snowmelt are identified via the linear regression method in any 30-year moving window in the record period. For peak runoff timing (QP), both methods show significant changes in a few 30-year windows for inflow to Millerton Lake (FRAC1), Pine Flat Reservoir (PFTC1), and Lake Success (SCSC1). Furthermore, out of 21 possible 30-year windows from 1961–2010, one sub-period 1971–2000 shows earlier peak in inflow to New Melones Reservoir (NMSC1) and two sub-periods (1969–1998 and 1971–2000) show earlier inflow peak for Lake Isabella (ISAC1) when the MKT method is applied. As for the timing of the center of mass of the annual runoff (QC), both methods identified two sub-periods (1980–2009 and 1981–2010) for Lake Oroville (ORDC1) and Folsom Lake (FOLC1) that show significant changes. For peak snowmelt timing, no methods show any significant changes in four out of 12 reservoirs. However, for Lake Isabella (ISAC1), both methods identify earlier peaks in 11 sub-periods. Note when looking at the entire record period, ISAC1 is the only location showing significant ($\alpha = 0.10$) earlier peaks in snowmelt when the linear regression and the MKT (with and without using the pre-whitening procedure) are applied.

Table 8. Number of 30-year periods showing significant trends via the MKT and linear regression methods ¹.

ID	Q1D	Q3D	Q5D	S1D	S3D	S5D	QP	QC	SP
SHDC1	0/0	0/0	0/0	0/0	0/0	0/0	0/0	0/0	0/0
ORDC1	0/0	0/0	0/0	0/0	0/0	0/0	0/0	2/2	0/0
HLEC1	0/0	0/0	0/0	0/0	0/0	0/0	0/0	0/0	0/0
FOLC1	0/0	0/0	0/0	0/0	1/0	2/0	0/0	2/2	0/0
NMSC1	0/0	0/0	0/0	1/0	1/0	0/0	1/0	0/0	0/0
NDPC1	0/0	0/0	0/0	0/0	0/0	0/0	0/0	0/0	0/0
EXQC1	0/0	0/0	0/0	0/0	0/0	0/0	0/0	0/0	0/0
FRAC1	0/0	0/0	0/0	0/0	0/0	0/0	2/2	0/0	4/3
PFTC1	0/0	0/0	0/0	0/0	0/0	0/0	3/3	0/0	0/0
TMDC1	0/0	0/0	0/0	0/0	0/0	0/0	0/0	0/0	1/1
SCSC1	0/0	0/0	0/0	0/0	0/0	0/0	2/4	0/0	0/2
ISAC1	0/0	0/0	0/0	0/0	0/0	0/0	2/0	0/0	11/11

¹ The first and second number represent results for the MKT and linear regression methods, respectively.

All in all, no wide spread significant changes in inflows to the 12 study Reservoirs are identified in this study. Similar findings have also been reported in the literature. For instance, Tamaddun et al. [60] investigated changes in unimpaired streamflow measured at 600 USGS stations (including 40 in California) across the Continental United States at the annual and seasonal scales. They identified no significant trends in annual and spring streamflow volumes at any of those 40 California stations via the MKT method either with or without the pre-whitening procedure incorporated. They used a significance level at 0.10 rather than 0.05. In the current study, the lack of significant trend in runoff extremes may attribute to the lack of widespread changes in precipitation extremes (Table 4 and Figure 8). It is also worth noting that the unimpaired runoff is calculated based on streamflow observations as well as the forecasters' best knowledge on upstream regulations. Evaporation from reservoirs is typically neglected from the calculation. Fine-tuning the equations determining unimpaired reservoir inflow is an on-going effort of the forecasters. A follow-up study will be conducted and reported when the updated dataset is available.

4.4. Implications of This Study

The study is unique in that it uses the operational dataset exclusively. These data are quality controlled by the forecasters based on their knowledge of the natural characteristics of the study areas as well as diversions and regulations in those areas. Real-time decisions on water management planning and management operations in the Central Valley are directly based on these data. The findings of this study have both scientific and practical significance.

From a scientific perspective, increasing warm extremes observed in certain areas in the Central Valley can guide the enhancement of the current forecasting model specifically for those areas. For instance, the current snow forecasting model SNOW-17 [61] uses a parameter to represent the maximum possible snow melt rate. The parameter is typically determined from historical temperature data. In light of the increasing warm extremes, the actual snow melt rate is most likely to increase accordingly. As such, this parameter needs to be refined to better reflect the new reality and thus provide more skillful forecasting. Another area for enhancement is developing new snow accumulation and ablation processes and incorporating them to the operational forecasting model. The current model is built on snow measurements available about four decades ago [61] when anthropogenic change of climate was not as substantial and the stationarity assumption may still have been sound. In the past several decades, significant changes in snowpack volume have been recorded in the Sierra Nevada Mountains [62–64] and are projected to continue to change in the future [65]. Snow monitoring techniques have also evolved and advanced significantly, providing more comprehensive data sources which likely revolutionize the snow sciences [66–69]. How to capitalize on these advancements to modernize our forecasting tools remains to be a challenging task for (particularly the next generation) forecasters.

From a practical perspective, these findings have significant implications for adaptive water resources planning and management practices. For example, the current reservoir operation rule curves in the Central Valley are mostly built on historical record of runoff, precipitation, and temperature with the assumption being no changes in those variables, while this study shows increasing warm extremes in a range of areas across the Central Valley. The warming trend is projected to continue [70–72], mostly likely leading to increased flooding risks [73,74] and more precipitation falling as rainfall instead of snowfall [75,76]. The traditional operation rules need to be updated accordingly to better manage water resources to satisfy increasing and often competing demands in California. Potential changes to the current rule curves may include reserving a larger flood pool and adjusting the top of conservation pool downward throughout the winter. Additionally, identifying the vulnerability of the current water system (including both natural watersheds and man-made water transfer and storage systems including the SWP and CVP) to a changing climate is the foremost step in developing and implementing any adaptation strategies [77]. This study shows that Tulare region observes the most significant warming among all six study regions in the Central Valley, suggesting that it is highly vulnerable to climate change and requires timely adaptation and mitigation responses.

5. Conclusions

This study presents a comprehensive trend analysis of temperature, precipitation, and runoff extremes in the Central Valley of California using available long-term operational datasets. Overall, this study highlights that Central Valley's precipitation, temperature, and runoff extremes are not immune from a globally changing climate. Specifically, about 60% of the study area shows increasing warm extremes and decreasing cold extremes. In comparison, changes in precipitation extremes are not as widespread. Only four out of nine precipitation indices show significant trends in a limited number (ranging from 4–22 out of 176) of basins. As for runoff, only one study location (out of 12) shows significant earlier snowmelt peak timing. Additional analysis on runoff indices using different trend analysis methods and different analysis periods also indicates limited changes in these runoff indices. These findings are meaningful in term of guiding water resources planning and management operations (e.g., prioritizing investment towards the most vulnerable region) and enhancing our forecasting tools for improved hydrologic forecasts.

Acknowledgments: The authors thank two anonymous reviewers for their constructive comments which helped improve the quality of the study. The authors would like to thank Mahesh Gautam in providing Matlab scripts for the trend analysis. The authors also want to thank John Andrew for his management support on the study. Any findings, opinions, and conclusions expressed in this paper are solely the authors' and do not reflect the views or opinions of their employers.

Author Contributions: The study was conceived by the authors together. The lead author (M.H.) conducted the study and wrote the paper. P.F. and B.W. produced and conducted quality control of the data. M.R., M.A., A.S., and E.L. provided critical discussions.

Conflicts of Interest: The authors declare no conflict of interest.

Appendix

The Appendix provides detailed information on the location of 176 study basins in six forecasting groups (Figure 1A) as well as the basic information for them (Tables A1–A6).

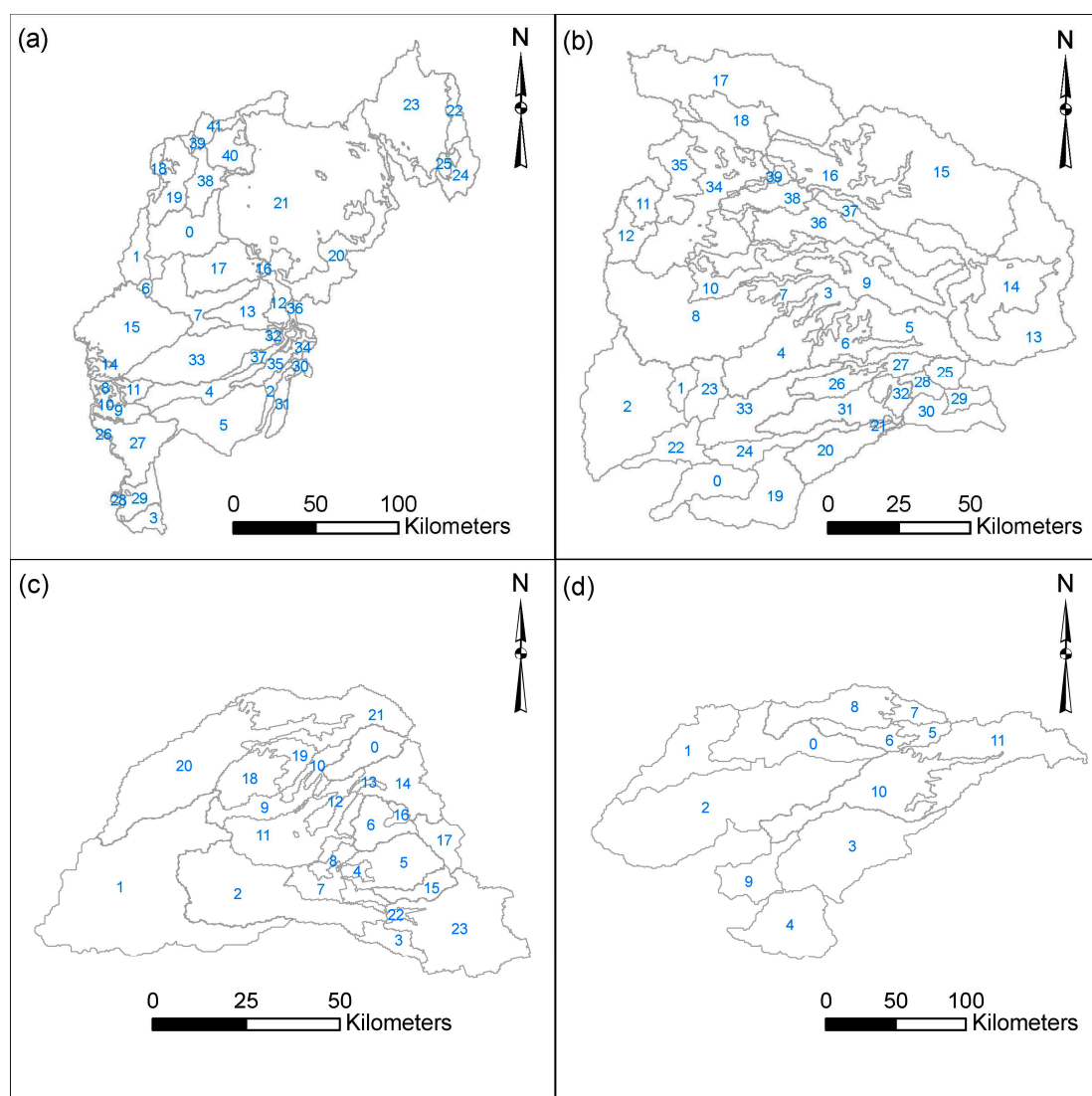


Figure A1. Cont.

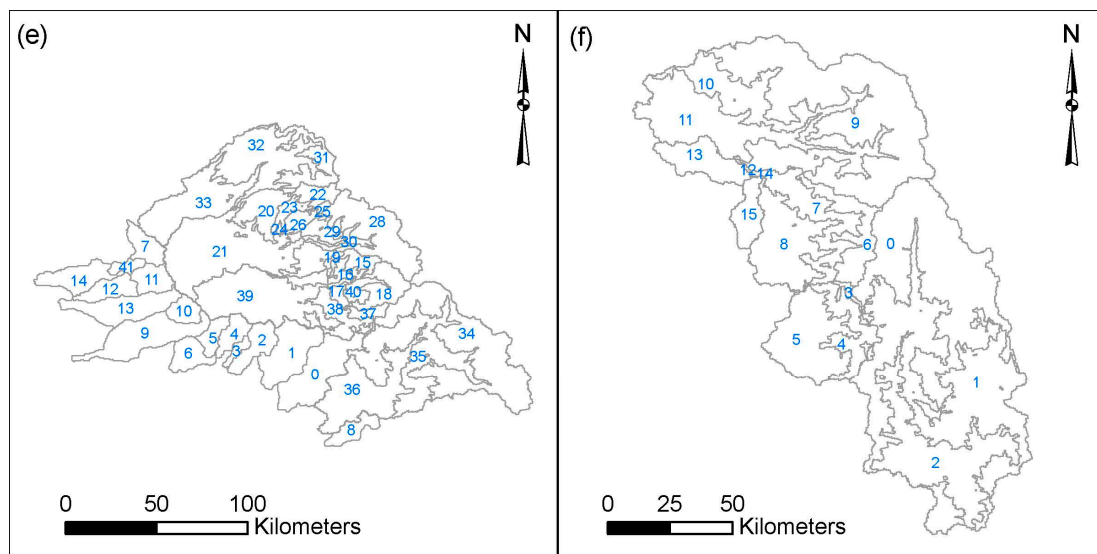


Figure A1. Study basins of (a) Upper Sacramento Group; (b) Feather Yuba Group; (c) American Group; (d) North San Joaquin Group; (e) San Joaquin Group and (f) Tulare Group.

Table A1. Study basins in the Upper Sacramento Group.

No.	ID	Description	Elevation (m)	Area (km ²)
0	SHDC1LOF	Sacramento River-Shasta Lake	579	1126
1	WHSC1HOF	Whiskeytown Dam	1067	512
2	HKCC1HOF	Big Chico Creek-Chico	950	184
3	EPRC1HOF	Little Stony Creek-East Park Reservoir	549	251
4	VWBC1LOF	Sacramento River-Vina Woodson Bridge	347	586
5	ORFC1LOF	Sacramento River-Ord Ferry	107	1562
6	RDGC1LOF	Clear Creek Near Igoca	243	72
7	BDBC1LOF	Sacramento River-Bend Bridge	243	1267
8	TCRC1HUF	Thomes Creek-Paskenta Upper	1723	177
9	TCRC1HLF	Thomes Creek-Paskenta Lower	1112	343
10	EDCC1HUF	Elder Creek-Paskenta Upper	1670	35
11	EDCC1HLF	Elder Creek-Paskenta Lower	677	201
12	COTC1HUF	Battle Creek-Cottonwood Upper	1790	302
13	COTC1HLF	Battle Creek-Cottonwood Lower	973	612
14	CWAC1HUF	Cottonwood Creek-Cottonwood Upper	1676	166
15	CWAC1HLF	Cottonwood Creek-Cottonwood Lower	480	2207
16	CWCC1HUF	Cow Creek-Millville Upper	1676	87
17	CWCC1HLF	Cow Creek-Millville Lower	480	1001
18	DLTC1HUF	Sacramento River-Delta Upper	1783	283
19	DLTC1HLF	Sacramento River-Delta Lower	1052	805
20	PITC1LUF	Pit River-Montgomery Creek Upper	1798	1893
21	PITC1LLF	Pit River-Montgomery Creek Lower	1311	7121
22	CNBC1LUF	Pit River-Canby Upper	1890	637
23	CNBC1LLF	Pit River-Canby Lower	1496	2395
24	PLYC1HUF	Sout Fork Pit River-Likely Upper	2151	500
25	PLYC1HLF	Sout Fork Pit River-Likely Lower	1585	133
26	BLBC1LUF	Stony Creek-Black Butte Reservoir Upper	1685	79
27	BLBC1LLF	Stony Creek-Black Butte Reservoir Lower	590	1048
28	SGEC1LUF	Stony Creek-Stony Gorge Reservoir Upper	1681	62
29	SGEC1LLF	Stony Creek-Stony Gorge Reservoir Lower	541	457
30	BKCC1HUF	Butte Creek Near Chico Upper	1680	105
31	BKCC1HLF	Butte Creek Near Chico Lower	819	271

Table A1. Cont.

No.	ID	Description	Elevation (m)	Area (km ²)
32	TEHC1LUF	Sacramento River-Tehama Bridge Upper	1722	27
33	TEHC1LLF	Sacramento River-Tehama Bridge Lower	347	1310
34	DCVC1HUF	Deer Creek-Vina Upper	1680	181
35	DCVC1HLF	Deer Creek-Vina Lower	819	351
36	MLMC1HUF	Mill Creek-Los Molinos Upper	1722	114
37	MLMC1HLF	Mill Creek-Los Molinos Lower	792	221
38	MSSC1LLF	Mccloud River-Shasta Lake Lower	1722	69
39	MSSC1LUF	Mccloud River-Shasta Lake Upper	1067	560
40	MMCC1HLF	Mccloud River-Mccloud Lower	1250	577
41	MMCC1HUF	Mccloud River-Mccloud Upper	1798	339

Table A2. Study basins in the Feather Yuba Group.

No.	ID	Description	Elevation (m)	Area (km ²)
0	DCWC1HOF	Wheatland Dry Creek	222	256
1	HCTC1HOF	South Fork Honcut Creek Nr Bangor	514	78
2	YUBC1LOF	Feather River-Yuba City	59	763
3	NBBC1LUF	North Fork Yuba River-New Bullards Bar Reservoir Upper	1692	159
4	NBBC1LLF	North Fork Yuba River-New Bullards Bar Reservoir Lower	1063	453
5	GYRC1HUF	North Yuba River Below Goodyears Bar Upper	1920	442
6	GYRC1HLF	North Yuba River Below Goodyears Bar Lower	1280	198
7	ORDC1LUF	Feather River-Lake Oroville Upper	1676	199
8	ORDC1LLF	Feather River-Lake Oroville Lower	815	1047
9	MRMC1LUF	Merrimac Middle Fork Feather Upper	1745	731
10	MRMC1LLF	Merrimac Middle Fork Feather Lower	1347	487
11	WBG1HUF	West Branch Feather River- Magalia Upper	1750	113
12	WBG1HLF	West Branch Feather River- Magalia Lower	1062	156
13	MFTC1HUF	Middle Fork Feather River-Portola Upper	1849	1127
14	MFTC1HLF	Middle Fork Feather River-Portola Lower	1521	376
15	IIFC1HUF	Indian Falls Indian Creek Upper	1810	1476
16	IIFC1HLF	Indian Falls Indian Creek Lower	1200	416
17	PLLC1HUF	North Fork Feather River-Prattville Upper	1788	1006
18	PLLC1HLF	North Fork Feather River-Prattville Lower	1418	251
19	CFWC1LOF	Bear River-Camp Far West Reservoir	526	451
20	ROLC1HLF	Bear River-Rollins Lake Lower	980	253
21	ROLC1HUF	Bear River-Rollins Lake Upper	1608	13
22	MRYC1LOF	Marysville Yuba	137	187
23	DMCC1HOF	Dry Creek-Merle Collins Reservoir	671	183
24	DCSC1HOF	Deer Creek-Smartsville	693	170
25	JKRC1HOF	Middle Fork Yuba River-Jackson Meadows Reservoir	2088	96
26	OURC1LLF	Middle Fork Yuba River-Our House Lower	913	159
27	OURC1LUF	Middle Fork Yuba River-Our House Upper	1813	115
28	BWKC1HOF	Canyon Creek-Bowman Reservoir	2027	69
29	FOCC1HOF	Fordyce Creek-Fordyce Lake	2217	81
30	SUAC1LOF	South Fork Yuba River-Lake Spaulding	2027	221
31	JNSC1LLF	South Fork Yuba River-Jones Bar Lower	1052	305
32	JNSC1LUF	South Fork Yuba River-Jones Bar Upper	1753	113
33	HLEC1LOF	Yuba River-Englebright Reservoir	640	425
34	PLGC1LLF	North Fork Feather River At Pulga Lower	1092	626
35	PLGC1LUF	North Fork Feather River At Pulga Upper	1745	492
36	SCBC1HLF	Spanish Creek-Keddie Lower	1280	306
37	SCBC1HUF	Spanish Creek-Keddie Upper	1781	165
38	NFEC1LLF	North Fork Feather River-East Branch Lower	1195	188
39	NFEC1LUF	North Fork Feather River-East Branch Upper	1676	73

Table A3. Study basins in the American Group.

No.	ID	Description	Elevation (m)	Area (km ²)
0	FMDC1HOF	French Meadows Reservoir Near Foresthill	1920	147
1	FOLC1LOF	American River-Folsom Lake	442	1016
2	CBAC1LLF	South Fork American River-Chili Bar Reservoir Lower	975	461
3	CBAC1LUF	South Fork American River-Chili Bar Reservoir Upper	1707	138
4	UNVC1HLF	Union Valley Reservoir Lower	1448	22
5	UNVC1HUF	Union Valley Reservoir Upper	1905	194
6	RRGC1HOF	South Fork Rubicon River Below Gerle Creek	1829	101
7	SVCC1LLF	Silver Creek-Camino Reservoir Lower	1402	81
8	SVCC1LUF	Silver Creek-Camino Reservoir Upper	1615	72
9	MFAC1LLF	Foresthill Middle Fork American River Lower	1097	106
10	MFAC1LUF	Foresthill Middle Fork American River Upper	1707	55
11	RUFC1LLF	Rubicon River Near Foresthill Upper	1250	274
12	RUFC1LUF	Rubicon River Near Foresthill Lower	1646	118
13	HLLC1LLF	Rubicon River-Hell Hole Reservoir Lower	1432	12
14	HLLC1LUF	Rubicon River-Hell Hole Reservoir Upper	2057	195
15	ICHC1HOF	South Fork Silver Creek-Ice House Reservoir	2088	70
16	LNLC1HOF	Loon Lake	1951	20
17	RBBC1HOF	Rubicon River-Rockbound Lake	2331	84
18	NMFC1HLF	North Fork Of Middle Fork American River-Foresthill Lower	1250	148
19	NMFC1HUF	North Fork Of Middle Fork American River-Foresthill Upper	1646	80
20	NFDC1HLF	North Fork American River-North Fork Dam Lower	1100	552
21	NFDC1HUF	North Fork American River-North Fork Dam Upper	1900	324
22	AKYC1HLF	South Fork American River Near Kyburz Lower	1371	20
23	AKYC1HUF	South Fork American River Near Kyburz Upper	2149	474

Table A4. Study basins in the North San Joaquin Group.

No.	ID	Description	Elevation (m)	Area (km ²)
0	MHBC1LOF	Cosumnes River-Michigan Bar	457	573
1	MCNC1LOF	Cosumnes River-Mcconnell	61	486
2	THTC1LOF	Mokelumne River-Benson Ferry	530	829
3	NHGC1HOF	Calaveras River-New Hogan Reservoir	580	127
4	FRGC1HOF	Littlejohns Creek-Farmington Reservoir	122	497
5	SOSC1HUF	Middle Fork Cosumnes River Nearr Somerset Upper	1744	104
6	SOSC1HLF	Middle Fork Cosumnes River Nearr Somerse Lower	1196	170
7	EDOC1HUF	North Fork Cosumnes River Nearr El Dorado Upper	1745	115
8	EDOC1HLF	North Fork Cosumnes River Nearr El Dorado Lower	1013	409
9	MSGC1LOF	Mormon Slough-Bellota	122	276
10	CMPC1HLF	Mokelumne River-Pardee Reservoir Lower	1052	666
11	CMPC1HUF	Mokelumne River-Pardee Reservoir Upper	2179	814

Table A5. Study basins in the San Joaquin Group.

No.	ID	Description	Elevation (m)	Area (km ²)
0	HIDC1HOF	Fresno River-Hensley Lake	732	604
1	BHNC1HOF	Chowchilla River-Buchanan Reservoir	478	602
2	MPAC1HOF	Mariposa Creek-Mariposa Reservoir	550	274
3	OWCC1HOF	Owens Creek-Owens Reservoir	366	66
4	BCKC1HOF	Bear Creek-Bear Reservoir	442	184
5	BNCC1HOF	Burns Creek-Burns Creek Reservoir	283	189
6	MEEC1LOF	Mckee Rd Bear Ck	98	243
7	KNFC1LOF	Stanislaus R Blo Goodwin Dam	317	195
8	LTDC1HOF	Friant Little Dry Ck	282	181
9	STVC1LOF	Merced River-Stevenson (Stvc1)	107	154
10	DSNC1HOF	Snelling Dry Ck	230	187
11	DRYC1HOF	Dry Creek At Crabtree Road	300	228
12	DCMC1LOF	Modesto Dry Ck	300	282
13	MDSC1LOF	Tuolumne River-Modesto (Mdsc1)	35	128
14	RIPC1LOF	Ripon Stanislaus	61	154

Table A5. Cont.

No.	ID	Description	Elevation (m)	Area (km ²)
15	POHC1LUF	Merced River-Yosemite At Pohono Bridge Upper	2500	161
16	POHC1LMF	Merced River-Yosemite At Pohono Bridge Middle	2100	176
17	POHC1LLF	Merced River-Yosemite At Pohono Bridge Lower	890	22
18	HPIC1HUF	Happy Isles Merced River Upper	2720	338
19	NDPC1LUF	Tuolumne River-New Don Pedro Reservoir Upper	2500	45
20	NDPC1LMF	Tuolumne River-New Don Pedro Reservoir Middle	2100	656
21	NDPC1LLF	Tuolumne River-New Don Pedro Reservoir Lower	900	1560
22	CHVC1HUF	Cherry Creek-Cherry Lake Upper	2650	171
23	CHVC1HMF	Cherry Creek-Cherry Lake Middle	2000	117
24	CHVC1HLF	Cherry Creek-Cherry Lake Lower	1450	12
25	LNRC1HUF	Eleanor Creek-Lake Eleanor Upper	2438	40
26	LNRC1HMF	Eleanor Creek-Lake Eleanor Middle	2000	150
27	LNRC1HLF	Eleanor Creek-Lake Eleanor Lower	1460	10
28	HETC1HUF	Tuolumne River-Hetch Hetchy Reservoir Upper	2819	228
29	HETC1HMF	Tuolumne River-Hetch Hetchy Reservoir Middle	2126	148
30	HETC1HLF	Tuolumne River-Hetch Hetchy Reservoir Lower	1280	24
31	NMSC1HUF	Stanislaus River-New Melones Reservoir Upper	2682	365
32	NMSC1HMF	Stanislaus River-New Melones Reservoir Middle	1966	621
33	NMSC1HLF	Stanislaus River-New Melones Reservoir Lower	884	840
34	FRAC1HUF	San Joaquin River-Millerton Reservoir Upper	2770	1803
35	FRAC1HMF	San Joaquin River-Millerton Reservoir Middle	2100	1342
36	FRAC1HLF	San Joaquin River-Millerton Reservoir Lower	890	1048
37	EXQC1LUF	Merced River-Exchequer Reservoir Upper	2500	128
38	EXQC1LMF	Merced River-Exchequer Reservoir Middle	2100	440
39	EXQC1LLF	Merced River-Exchequer Reservoir Lower	900	1265
40	HPIC1HMF	Happy Isles Merced River Middle	2000	125
41	OBBC1LOF	Stanislaus River-Orange Blossom	107	90

Table A6. Study basins in the Tulare Group.

No.	ID	Description	Elevation (m)	Area (km ²)
0	ISAC1HUF	Kern River-Lake Isabella Upper	2591	54
1	ISAC1HMF	Kern River-Lake Isabella Middle	1905	840
2	ISAC1HLF	Kern River-Lake Isabella Lower	1143	893
3	SCSC1HUF	Tule River-Lake Success Upper	2621	50
4	SCSC1HMF	Tule River-Lake Success Middle	1905	300
5	SCSC1HLF	Tule River-Lake Success Lower	793	649
6	TMDC1HUF	Kaweah River-Lake Kaweah Upper	2591	51
7	TMDC1HMF	Kaweah River-Lake Kaweah Middle	1905	51
8	TMDC1HLF	Kaweah River-Lake Kaweah Lower	1143	262
9	PFTC1HUF	Kings River-Pine Flat Reservoir Upper	3048	2095
10	PFTC1HMF	Kings River-Pine Flat Reservoir Middle	2042	1028
11	PFTC1HLF	Kings River-Pine Flat Reservoir Lower	890	830
12	MLPC1HUF	Piedra Mill Creek Upper	1685	13
13	MLPC1HLF	Piedra Mill Creek Lower	747	312
14	DLMC1HUF	Lemoncove Dry Creek Upper	1752	6
15	DLMC1HLF	Lemoncove Dry Creek Lower	762	188

References

1. Easterling, D.R.; Meehl, G.A.; Parmesan, C.; Changnon, S.A.; Karl, T.R.; Mearns, L.O. Climate extremes: Observations, modeling, and impacts. *Science* **2000**, *289*, 2068–2074. [[CrossRef](#)] [[PubMed](#)]
2. Changnon, S.A.; Pielke, R.A., Jr.; Changnon, D.; Sylves, R.T.; Pulwarty, R. Human factors explain the increased losses from weather and climate extremes. *Bull. Am. Meteorol. Soc.* **2000**, *81*, 437–442. [[CrossRef](#)]
3. Bouwer, L.M. Have disaster losses increased due to anthropogenic climate change? *Bull. Am. Meteorol. Soc.* **2011**, *92*, 39–46. [[CrossRef](#)]

4. Nutter, F.W. Global climate change: Why U.S. Insurers care. In *Weather and Climate Extremes*; Springer: Dordrecht, The Netherlands, 1999; pp. 45–49.
5. Su, B.; Jiang, T.; Jin, W. Recent trends in observed temperature and precipitation extremes in the Yangtze River Basin, China. *Theor. Appl. Climatol.* **2006**, *83*, 139–151. [[CrossRef](#)]
6. Mora, C.; Dousset, B.; Caldwell, I.R.; Powell, F.E.; Geronimo, R.C.; Bielecki, C.R.; Counsell, C.W.; Dietrich, B.S.; Johnston, E.T.; Louis, L.V. Global risk of deadly heat. *Nat. Clim. Chang.* **2017**, *7*, 501–506. [[CrossRef](#)]
7. AghaKouchak, A.; Cheng, L.; Mazdiyasi, O.; Farahmand, A. Global warming and changes in risk of concurrent climate extremes: Insights from the 2014 California drought. *Geophys. Res. Lett.* **2014**, *41*, 8847–8852. [[CrossRef](#)]
8. Yoon, J.-H.; Wang, S.S.; Gillies, R.R.; Kravitz, B.; Hippias, L.; Rasch, P.J. Increasing water cycle extremes in California and in relation to ENSO cycle under global warming. *Nat. Commun.* **2015**, *6*, 8657. [[CrossRef](#)] [[PubMed](#)]
9. Berg, N.; Hall, A. Increased interannual precipitation extremes over California under climate change. *J. Clim.* **2015**, *28*, 6324–6334. [[CrossRef](#)]
10. Alexander, L.; Zhang, X.; Peterson, T.; Caesar, J.; Gleason, B.; Tank, A.K.; Haylock, M.; Collins, D.; Trewin, B.; Rahimzadeh, F. Global observed changes in daily climate extremes of temperature and precipitation. *J. Geophys. Res. Atmos.* **2006**, *111*. [[CrossRef](#)]
11. He, M.; Gautam, M. Variability and trends in precipitation, temperature and drought indices in the State of California. *Hydrology* **2016**, *3*, 14. [[CrossRef](#)]
12. Peterson, T.C.; Taylor, M.A.; Demeritte, R.; Duncombe, D.L.; Burton, S.; Thompson, F.; Porter, A.; Mercedes, M.; Villegas, E.; Fils, R.S. Recent changes in climate extremes in the Caribbean region. *J. Geophys. Res. Atmos.* **2002**, *107*, 4601. [[CrossRef](#)]
13. Easterling, D.R.; Evans, J.; Groisman, P.Y.; Karl, T.R.; Kunkel, K.E.; Ambenje, P. Observed variability and trends in extreme climate events: A brief review. *Bull. Am. Meteorol. Soc.* **2000**, *81*, 417–425. [[CrossRef](#)]
14. Vincent, L.A.; Peterson, T.; Barros, V.; Marino, M.; Rusticucci, M.; Carrasco, G.; Ramirez, E.; Alves, L.; Ambrizzi, T.; Berlato, M. Observed trends in indices of daily temperature extremes in South America 1960–2000. *J. Clim.* **2005**, *18*, 5011–5023. [[CrossRef](#)]
15. Haylock, M.R.; Peterson, T.; Alves, L.; Ambrizzi, T.; Anunciação, Y.; Baez, J.; Barros, V.; Berlato, M.; Bidegain, M.; Coronel, G. Trends in total and extreme South American rainfall in 1960–2000 and links with sea surface temperature. *J. Clim.* **2006**, *19*, 1490–1512. [[CrossRef](#)]
16. Zhang, X.; Aguilar, E.; Sensoy, S.; Melkonyan, H.; Tagiyeva, U.; Ahmed, N.; Kotaladze, N.; Rahimzadeh, F.; Taghipour, A.; Hantosh, T. Trends in Middle East climate extreme indices from 1950 to 2003. *J. Geophys. Res. Atmos.* **2005**, *110*. [[CrossRef](#)]
17. Aguilar, E.; Barry, A.A.; Brunet, M.; Ekang, L.; Fernandes, A.; Massoukina, M.; Mbah, J.; Mhanda, A.; Do Nascimento, D.; Peterson, T. Changes in temperature and precipitation extremes in western Central Africa, Guinea Conakry, and Zimbabwe, 1955–2006. *J. Geophys. Res. Atmos.* **2009**, *114*. [[CrossRef](#)]
18. United States Census Bureau. 2010 Census Summary File 1. Available online: <https://www.census.gov/2010census/data/> (accessed on 1 August 2017).
19. Dettinger, M.D.; Ralph, F.M.; Das, T.; Neiman, P.J.; Cayan, D.R. Atmospheric rivers, floods and the water resources of California. *Water* **2011**, *3*, 445–478. [[CrossRef](#)]
20. He, M.; Russo, M.; Anderson, M. Hydroclimatic characteristics of the 2012–2015 California drought from an operational perspective. *Climate* **2017**, *5*, 5. [[CrossRef](#)]
21. Chung, F.; Kelly, K.; Guivetchi, K. Averting a California water crisis. *J. Water Resour. Plan. Manag.* **2002**, *128*, 237–239. [[CrossRef](#)]
22. Pryor, S.; Howe, J.; Kunkel, K. How spatially coherent and statistically robust are temporal changes in extreme precipitation in the Contiguous USA? *Int. J. Climatol.* **2009**, *29*, 31–45. [[CrossRef](#)]
23. Grundstein, A.; Dowd, J. Trends in extreme apparent temperatures over the United States, 1949–2010. *J. Appl. Meteorol. Clim.* **2011**, *50*, 1650–1653. [[CrossRef](#)]
24. Grundstein, A. Evaluation of climate change over the continental United States using a moisture index. *Clim. Chang.* **2009**, *93*, 103–115. [[CrossRef](#)]
25. Schwartz, M.D.; Ault, T.R.; Betancourt, J.L. Spring onset variations and trends in the continental United States: Past and regional assessment using temperature-based indices. *Int. J. Climatol.* **2013**, *33*, 2917–2922. [[CrossRef](#)]

26. Bonfils, C.; Duffy, P.B.; Santer, B.D.; Wigley, T.M.; Lobell, D.B.; Phillips, T.J.; Doutriaux, C. Identification of external influences on temperatures in California. *Clim. Chang.* **2008**, *87*, 43–55. [[CrossRef](#)]
27. Caroni, C.; Panagoulia, D.; Economou, P. Non-stationary modelling of extremes of precipitation and temperature over mountainous areas under climate change. In Proceedings of the International Conference in Current Topics on Risk Analysis, Barcelona, Spain, 26–29 May 2015; pp. 203–209.
28. Panagoulia, D.; Economou, P.; Caroni, C. Stationary and nonstationary generalized extreme value modelling of extreme precipitation over a mountainous area under climate change. *Environmetrics* **2014**, *25*, 29–43. [[CrossRef](#)]
29. Daly, C. Climate division normals derived from topographically-sensitive climate grids. In Proceedings of the 13th AMS Conference on Applied Climatology, Portland, OR, USA, 13–16 May 2002; pp. 177–180.
30. Smith, M.B.; Laurine, D.P.; Koren, V.I.; Reed, S.M.; Zhang, Z. Hydrologic model calibration in the National Weather Service. In *Calibration of Watershed Models*; Wiley: Washington, DC, USA, 2003; pp. 133–152.
31. Peterson, T.; Folland, C.; Gruza, G.; Hogg, W.; Mokssit, A.; Plummer, N. *Report on the Activities of the Working Group on Climate Change Detection and Related Rapporteurs*; World Meteorological Organization: Geneva, Switzerland, 2001.
32. Wang, W.; Shao, Q.; Yang, T.; Peng, S.; Yu, Z.; Taylor, J.; Xing, W.; Zhao, C.; Sun, F. Changes in daily temperature and precipitation extremes in the Yellow River Basin, China. *Stoch. Environ. Res. Risk Assess.* **2013**, *27*, 401–421. [[CrossRef](#)]
33. Vincent, L.; Aguilar, E.; Saindou, M.; Hassane, A.; Jumaux, G.; Roy, D.; Booneeady, P.; Virasami, R.; Randriamarolaza, L.; Faniriantsoa, F. Observed trends in indices of daily and extreme temperature and precipitation for the countries of the Western Indian Ocean, 1961–2008. *J. Geophys. Res. Atmos.* **2011**, *116*. [[CrossRef](#)]
34. New, M.; Hewitson, B.; Stephenson, D.B.; Tsiga, A.; Kruger, A.; Manhique, A.; Gomez, B.; Coelho, C.A.; Masisi, D.N.; Kululanga, E. Evidence of trends in daily climate extremes over southern and west Africa. *J. Geophys. Res. Atmos.* **2006**, *111*. [[CrossRef](#)]
35. Tank, A.K.; Peterson, T.; Quadir, D.; Dorji, S.; Zou, X.; Tang, H.; Santhosh, K.; Joshi, U.; Jaswal, A.; Kolli, R. Changes in daily temperature and precipitation extremes in central and south Asia. *J. Geophys. Res. Atmos.* **2006**, *111*. [[CrossRef](#)]
36. California Department of Water Resources. Central Valley Flood Protection Plan 2017 Update. Available online: <http://www.water.ca.gov/cvfmp/docs/2017/2017CVFPPUpdate-Final-20170828.pdf> (accessed on 1 October 2017).
37. Stewart, I.T.; Cayan, D.R.; Dettinger, M.D. Changes in snowmelt runoff timing in western North America under a business-as-usual climate change scenario. *Clim. Chang.* **2004**, *62*, 217–232. [[CrossRef](#)]
38. Stewart, I.T.; Cayan, D.R.; Dettinger, M.D. Changes toward earlier streamflow timing across western North America. *J. Clim.* **2005**, *18*, 1136–1155. [[CrossRef](#)]
39. Hirsch, R.M.; Helsel, D.; Cohn, T.; Gilroy, E. Statistical analysis of hydrologic data. *Handb. Hydrol.* **1993**, *17*, 11–55.
40. Helsel, D.R.; Hirsch, R.M. *Statistical Methods in Water Resources*; Elsevier: Amsterdam, The Netherlands, 1992; Volume 49.
41. Mann, H. Non-parametric tests against trend. *Econometrica* **1945**, *13*, 245–259. [[CrossRef](#)]
42. Kendall, M.G. *Rank Correlation Methods*; Charles Griffin: London, UK, 1975.
43. Yue, S.; Pilon, P.; Phinney, B.; Cavadias, G. The influence of autocorrelation on the ability to detect trend in hydrological series. *Hydrol. Process.* **2002**, *16*, 1807–1829. [[CrossRef](#)]
44. Thiel, H. A rank-invariant method of linear and polynomial regression analysis, part 3. *Proc. Koninklijke Ned. Akad. Wetensch. A* **1950**, *53*, 1397–1412.
45. Sen, P.K. Estimates of the regression coefficient based on Kendall's tau. *J. Am. Stat. Assoc.* **1968**, *63*, 1379–1389. [[CrossRef](#)]
46. Von Storch, H. Misuses of statistical analysis in climate research. In *Analysis of Climate Variability*; Springer: Berlin/Heidelberg, Germany, 1995; pp. 11–26.
47. Douglas, E.; Vogel, R.; Kroll, C. Trends in floods and low flows in the United States: Impact of spatial correlation. *J. Hydrol.* **2000**, *240*, 90–105. [[CrossRef](#)]
48. Hamed, K.H.; Rao, A.R. A modified Mann-Kendall trend test for autocorrelated data. *J. Hydrol.* **1998**, *204*, 182–196. [[CrossRef](#)]

49. Yue, S.; Pilon, P.; Phinney, B. Canadian streamflow trend detection: Impacts of serial and cross-correlation. *Hydrol. Sci. J.* **2003**, *48*, 51–63. [[CrossRef](#)]
50. Massey, F.J., Jr. The Kolmogorov-Smirnov test for goodness of fit. *J. Am. Stat. Assoc.* **1951**, *46*, 68–78. [[CrossRef](#)]
51. Qin, N.; Chen, X.; Fu, G.; Zhai, J.; Xue, X. Precipitation and temperature trends for the southwest China: 1960–2007. *Hydrol. Process.* **2010**, *24*, 3733–3744. [[CrossRef](#)]
52. Soro, G.E.; Noufé, D.; Goula Bi, T.A.; Shorohou, B. Trend analysis for extreme rainfall at sub-daily and daily timescales in Côte d'Ivoire. *Climate* **2016**, *4*, 37. [[CrossRef](#)]
53. Attogouinon, A.A.; Lawin, A.E.; M'Po, Y.N.T.; Houngue, R. Extreme precipitation indices trend assessment over the upper Ueme River Valley (Benin). *Hydrology* **2017**, *4*, 36. [[CrossRef](#)]
54. Regonda, S.K.; Rajagopalan, B.; Clark, M.; Pitlick, J. Seasonal cycle shifts in hydroclimatology over the western United States. *J. Clim.* **2005**, *18*, 372–384. [[CrossRef](#)]
55. McCabe, G.J.; Clark, M.P. Trends and variability in snowmelt runoff in the western United States. *J. Hydrometeorol.* **2005**, *6*, 476–482. [[CrossRef](#)]
56. Hidalgo, H.; Das, T.; Dettinger, M.; Cayan, D.; Pierce, D.; Barnett, T.; Bala, G.; Mirin, A.; Wood, A.; Bonfils, C. Detection and attribution of streamflow timing changes to climate change in the western United States. *J. Clim.* **2009**, *22*, 3838–3855. [[CrossRef](#)]
57. Dudley, R.; Hodgkins, G.; McHale, M.; Kolian, M.; Renard, B. Trends in snowmelt-related streamflow timing in the Conterminous United States. *J. Hydrol.* **2017**, *547*, 208–221. [[CrossRef](#)]
58. Burn, D.H. Climatic influences on streamflow timing in the headwaters of the Mackenzie River Basin. *J. Hydrol.* **2008**, *352*, 225–238. [[CrossRef](#)]
59. Lins, H.F.; Slack, J.R. Streamflow trends in the United States. *Geophys. Res. Lett.* **1999**, *26*, 227–230. [[CrossRef](#)]
60. Tamaddun, K.; Kalra, A.; Ahmad, S. Identification of streamflow changes across the Continental United States using variable record lengths. *Hydrology* **2016**, *3*, 24. [[CrossRef](#)]
61. Anderson, E.A. *National Weather Service River Forecast System—Snow Accumulation and Ablation Model*; Technical Memorandum NWS HYDRO-17, November 1973; NOAA: Washington, DC, USA, 1973; p. 217.
62. Mote, P.W.; Hamlet, A.F.; Clark, M.P.; Lettenmaier, D.P. Declining mountain snowpack in western North America. *Bull. Am. Meteorol. Soc.* **2005**, *86*, 39–49. [[CrossRef](#)]
63. Mote, P.W. Trends in snow water equivalent in the Pacific Northwest and their climatic causes. *Geophys. Res. Lett.* **2003**, *30*. [[CrossRef](#)]
64. Kapnick, S.; Hall, A. Observed climate–snowpack relationships in California and their implications for the future. *J. Clim.* **2010**, *23*, 3446–3456. [[CrossRef](#)]
65. Sun, F.; Hall, A.; Schwartz, M.; Walton, D.B.; Berg, N. Twenty-first-century snowfall and snowpack changes over the southern California mountains. *J. Clim.* **2016**, *29*, 91–110. [[CrossRef](#)]
66. Painter, T.; Berisford, D.; Boardman, J.; Bormann, K.; Deems, J.; Gehrke, F.; Hedrick, A.; Joyce, M.; Laidlaw, R.; Marks, D. The airborne snow observatory: Scanning lidar and imaging spectrometer fusion for mapping snow water equivalent and snow albedo. *Remote Sens. Environ.* **2016**, *184*, 139–152. [[CrossRef](#)]
67. Seidel, F.C.; Rittger, K.; Skiles, S.; Molotch, N.P.; Painter, T.H. Case study of spatial and temporal variability of snow cover, grain size, albedo and radiative forcing in the Sierra Nevada and rocky mountain snowpack derived from imaging spectroscopy. *Cryosphere* **2016**, *10*, 1229–1244. [[CrossRef](#)]
68. Huning, L.S.; Margulis, S.A. Climatology of seasonal snowfall accumulation across the Sierra Nevada (USA): Accumulation rates, distributions, and variability. *Water Resour. Res.* **2017**. [[CrossRef](#)]
69. Sturm, M. White water: Fifty years of snow research in wrr and the outlook for the future. *Water Resour. Res.* **2015**, *51*, 4948–4965. [[CrossRef](#)]
70. Cayan, D.R.; Maurer, E.P.; Dettinger, M.D.; Tyree, M.; Hayhoe, K. Climate change scenarios for the California region. *Clim. Chang.* **2008**, *87*, 21–42. [[CrossRef](#)]
71. Dettinger, M.D. Projections and downscaling of 21st century temperatures, precipitation, radiative fluxes and winds for the southwestern US, with focus on Lake Tahoe. *Clim. Chang.* **2013**, *116*, 17–33. [[CrossRef](#)]
72. Scherer, M.; Diffenbaugh, N.S. Transient twenty-first century changes in daily-scale temperature extremes in the United States. *Clim. Dyn.* **2014**, *42*, 1383–1404. [[CrossRef](#)]
73. Das, T.; Dettinger, M.D.; Cayan, D.R.; Hidalgo, H.G. Potential increase in floods in California's Sierra Nevada under future climate projections. *Clim. Chang.* **2011**, *109*, 71–94. [[CrossRef](#)]

74. Das, T.; Maurer, E.P.; Pierce, D.W.; Dettinger, M.D.; Cayan, D.R. Increases in flood magnitudes in California under warming climates. *J. Hydrol.* **2013**, *501*, 101–110. [[CrossRef](#)]
75. Feng, S.; Hu, Q. Changes in winter snowfall/precipitation ratio in the Contiguous United States. *J. Geophys. Res. Atmos.* **2007**, *112*. [[CrossRef](#)]
76. Coats, R. Climate change in the Tahoe basin: Regional trends, impacts and drivers. *Clim. Chang.* **2010**, *102*, 435–466. [[CrossRef](#)]
77. Andrew, J.T.; Sauquet, E. Climate change impacts and water management adaptation in two mediterranean-climate watersheds: Learning from the Durance and Sacramento rivers. *Water* **2016**, *9*, 126. [[CrossRef](#)]



© 2017 by the authors. Licensee MDPI, Basel, Switzerland. This article is an open access article distributed under the terms and conditions of the Creative Commons Attribution (CC BY) license (<http://creativecommons.org/licenses/by/4.0/>).